REPORT DOCUMENTATION PAGE

Form Approved
OPM No. 0704-0188

1. AGENCY USE ONLY *(Leave Blank)*	2. REPORT DATE	3. REPORT TYPE AND DATES COVERED
	January 1997	Final Report Jun '96 - Dec '96

4. TITLE AND SUBTITLE
"Determination of Non-Linear Dynamic Aerodynamic Coefficients for Aircraft"
(SBIR N96-017)

5. FUNDING NUMBERS
N00019-96-C-2038

6. AUTHOR(S)
Brooke C. Smith
Gerald N. Malcolm

7. PERFORMING ORGANIZATION NAME(S) AND ADDRESS(ES)
Eidetics Corporation
3425 Lomita Blvd.
Torrance, CA 90505

8. PERFORMING ORGANIZATION REPORT NUMBER
TR97-001

9. SPONSORING/MONITORING AGENCY NAME(S) AND ADDRESS(ES)
Naval Air Systems Command
Mr. Robert Hanley
Code AIR-4.3.2.4
1421 Jefferson Davis Highway
Arlington, VA 22243-2417

SPONSORING/MONITORING AGENCY

11. SUPPLEMENTARY NOTES

12a. DISTRIBUTION/AVAILABILITY STATEMENT
Approved for Public Release, Distribution Unlimited

12b. DISTRIBUTION CODE
UL

13. ABSTRACT *(Maximum 200 words)*

In order to accurately predict the flight dynamics of fighter aircraft, a relatively complete data base for static and dynamic aerodynamics properties for a complete range of flight conditions is required. Since it is impossible to acquire a complete data base for all possible combinations of aircraft attitude and motion parameters, the available data base must be interpolated between test data points for conditions that were not specifically tested. This requires an aerodynamic math model representation - the means for interpolating and combining test data to provide the appropriate aerodynamics data. This Phase I study focused on finding new testing techniques to improve the ability to represent dynamic terms sufficiently to account for important nonlinearities with rotation rate and to recognize and accommodate significant effects of motion time history dependency. Water tunnel dynamic force and moment tests were conducted with single and multiple degrees of freedom of rotational motion on an F/A-18 model, and recent high-amplitude high-rate roll- oscillation wind tunnel experiments on a 65° delta wing model were reviewed with the objective of developing a new testing methodology for the future. A key element in this new approach is determining "critical states" in the flow field, often related to vortex breakdown phenomena, prior to performing dynamic tests.

14. SUBJECT TERMS
Fighter Aircraft,
SBIR Phase I, Dynamic Testing for Aerodynamic Coefficients

15. NUMBER OF PAGES
103

16. PRICE CODE

17. SECURITY CLASSIFICATION OF REPORT	18. SECURITY CLASSIFICATION OF THIS PAGE	19. SECURITY CLASSIFICATION OF ABSTRACT	20. LIMITATION OF ABSTRACT
Unclassified	Unclassified	Unclassified	UL

NSN 7540-01-280-5500

Standard Form 298, (Rev. 2-89)
Prescribed by ANSI Std. 239-18

TABLE OF CONTENTS

1.0 BACKGROUND/INTRODUCTION

In order to accurately predict the flight dynamic characteristics of any aircraft, one must acquire a relatively complete data base on the static and dynamic aerodynamic properties of the configuration over the range of flight conditions of interest, including Mach number, Reynolds number, angle of attack and sideslip, etc. It is impossible to acquire a data base for all combinations of aircraft attitude and motion parameters. Therefore, the available data base must be interpolated between test data points for conditions that were not specifically tested. In order to do this, the acquired aerodynamic test data must be represented by a mathematical model - the procedure for interpolating and combining test data to provide aerodynamics data for any combination of attitude and motion parameters. The methods for interpolating and combining data from available test procedures vary considerably, depending on the principal objectives of the application and the availability of data.

The most challenging aerodynamic data to acquire are the dynamic aerodynamic coefficients, whether they be from computational aerodynamics methods or from experimental measurements from test facilities with sub-scale models. In flight regimes where the significant flow phenomena are characterized by a single response time - usually associated with convection time - airloads exhibit small delays that tend to vary linearly with rate, allowing the representation of coefficients in terms of derivatives, typically determined by means of small amplitude oscillatory experiments in the rotational axis of interest. This condition is more or less satisfied in the absence of vortex breakdown, i.e. at low AOA where vortex breakdown occurs aft of lifting surfaces, and possibly at sufficiently high AOA where the flow is fully separated and vortices are no longer present.

In the intermediate range of AOA, where breakdown occurs over lifting surfaces, the much slower response time of the breakdown motion results in the addition of important time delays in the airloads as a function of motion variables that cannot be linearly modeled. Furthermore, significant transients occur when crossing the boundary between the two regimes that cannot be represented by a linear model. Under these conditions more sophisticated methods must be used for modeling purposes, which have the ability to reflect the crucial motion history effects exhibited by the airloads

Modern fighter aircraft are also capable of producing maneuvers where the predominant rotational motion is not necessarily around one of the body axes, but, instead, is around the velocity vector at substantial angles of attack and sideslip. In this case, for example, the experimental test technique for acquiring data that best characterizes this motion is a rotary-balance test. The rotary-balance

apparatus allows the measurements of all six components of forces and moments on a model which is fixed at desired angles of attack and sideslip and rotated around the velocity vector over a range of constant rates scaled to be consistent with those expected for a full-scale aircraft.

Aerodynamic coefficients can also be measured in experiments consisting of high-amplitude harmonic motions, transient ramp motions and continuous rotation in one direction. The most difficult challenge is to use the experimental results in a meaningful and practical way to model the dynamic aerodynamic characteristics in general.

In addition to wind tunnel tests, aerodynamic data can also be extracted from sub- and full-scale flight tests through various techniques of parameter identification, but flight tests are usually not possible until quite late in the development of new configurations. Flight test data, then, is of most value in building up a verified simulation math model and for adjustments to control system parameters. Extracting aerodynamic data from flight tests requires analysis of the time history measurements of all of the flight state variables including angle of attack and sideslip, rotational and translational rates and accelerations, and an assumption of the form of the aerodynamic mathematical model which provides the framework to acquire specified static and dynamic aerodynamic coefficients.

All of these test techniques, ground-based and flight-based, are in general use to achieve the best possible representation for the airframe rotational and translational aerodynamic coefficients. The success in correlating predicted or simulated flight dynamics to actual flight dynamics is directly dependent on the choice of the aerodynamic math model and the ability to determine the appropriate values of the coefficients that comprise the mathematical model.

2.0 AERODYNAMIC MATHEMATICAL MODELS

Selection of the appropriate aerodynamic mathematical model and evaluation of the aerodynamic coefficients to represent full-scale aircraft flight is a formidable task. One must have a clear understanding of the difficulties in specifying a universal aerodynamic math model that has all of the required static and dynamic coefficients and the knowledge of what is required to determine them experimentally (or computationally when possible). Clearly the most important difficulty in properly predicting the dynamics of flight vehicles has been the inability to adequately model the aerodynamic terms in the equations of motion in a form that the chosen coefficients can a) be determined by existing experimental techniques and b) be properly combined to reflect the effect of a variety of complex motions encountered in the maneuvering regime. Proposing potential

improvements to this process requires both an assessment of the dynamic terms that typically have significant influence on the dynamic response of the aircraft and an insight of the flow phenomena underlying the behavior of these terms in the nonlinear regime. Furthermore, it is necessary to have an understanding of experimental methods used to obtain dynamic coefficients, particularly insofar as the relevance of the test conditions which in turn have a direct impact on the applicability of the test results to actual flight. Likewise, an understanding of the limitations of current test hardware and wind tunnel facilities is needed to have an adequate appreciation of the quality of test results.

Examples of existing methods of measuring and using aerodynamic coefficient data with several well-known and documented aero-math models for fighter aircraft are described in Ref. 1. Various aero-math models are discussed by Kalviste in Refs. 2-4. Some of these aerodynamic math models will be discussed briefly in Section 2.3. With an understanding of present methods of acquiring and reducing experimental dynamic aerodynamic data and how they are applied to existing aero-math for flight simulation, improved methods for conducting experiments can be explored, which is the main theme of this Phase I study.

2.1 Aero-Math Models - Where Do We Start?

All aero-math models are based on a variety of assumptions in order to simplify the final form sufficiently for practical application and to require aerodynamic coefficients that can be evaluated, usually experimentally. It is instructive to understand the derivation of a mathematical model where a minimum of apriori assumptions are made about which aerodynamic terms to keep and which ones to eliminate. Once the equations are derived with relative completeness in the terms for the aerodynamic model, a judgment can be made, based on legitimate reasons, to drop unimportant or insignificant terms in order to simplify the model. The terms that are ultimately retained will depend to some extent on the configuration of interest and the experimental results.

2.2 Approach to Aero-Math Modeling

Maneuvers of modern fighter aircraft at high angles of attack involve high rate rolling motions about the velocity vector as well as rotation about body-fixed axes. A complete aero-math model is derived in Appendix A and is composed of a combination of terms including body-fixed rotational and translational terms (which could be transformed to a wind-axis reference system if necessary) and rotary-balance type terms. If, for example, the motion in question is a pure rotation around the velocity vector, the applicable aerodynamic measurements would be those determined from a

rotary-balance rig. If the motion is a combination of steady rotation about the velocity vector and either oscillatory or ramp-type body-axis motions, the aerodynamic model will use coefficients from forced oscillation and rotary-balance measurements. How these coefficients from various experiments are to be combined to properly represent an actual 6-DOF motion is the key question.

The equations derived in Appendix A are developed to treat the most general case practical. The only basic assumption in the derivation of a "general" aero-math model is that it allows an arbitrary rotary motion to be decomposed into a velocity-vector roll component and components with residual body-axis rates. It is assumed that the form of the model consists of rotational motions about the three body axes, translational motions in the body vertical (z), and transverse (y) axes (no model motion in the body longitudinal or x-axis) and rotation around the velocity vector at a fixed model attitude. These motions have been chosen because they closely represent the components of actual flight motions and these specific motions are possible to perform in the wind tunnel, either individually or, in some cases, in combination simultaneously. Some typical practical aero-math models presently in use are discussed in Section 2.3.

2.3 Typical Aero-Math Model - Rotary-Balance and Oscillatory Components

Most aerodynamic math models that are currently used to represent the high-angle-of-attack flight dynamics of modern fighter aircraft are represented by a formulation that derives the aerodynamic coefficient information from rotary-balance and forced-oscillation wind tunnel tests. The actual form of the model and the related rational for combining the contributions from various experiments and the means of acquiring the data vary sufficiently throughout the aeronautical community that there is clearly no "common" methodology that always works best. There is a general consensus, however, that forced-oscillation data alone are completely inadequate. By the same token, unless the motion of interest is a steady spin or constant rotation about the velocity vector at fixed attitude, rotary-balance tests alone are also not adequate. The challenge is to find the best method of combining data from these two types of experiments so that the composite model provides an accurate representation of an arbitrary motion in flight. The issues that cloud the ability to "model" the aerodynamics are (1) nonlinearities in the data with respect to attitude and rotation rates, (2) effects of time history, i.e., large-amplitude versus small amplitude effects, and (3) the ability (or non-ability) to superpose results from separate experiments to create a true composite motion result. These issues are specifically discussed in Section 4.0. Examples of modeling techniques presently in use and their limitations are discussed in this section. These examples are typical of the aero-math models used by various organizations/experimenters to best represent the aerodynamics with present-day constraints in being able to perform only certain

dynamic experiments in the wind tunnel.

The preferred math model, of course, is one which has the widest range of applicability and accurately represents the aerodynamic characteristics of the aircraft that it is applied to. The most general form of the math model simply states that the right-hand side of the equations of motion, those terms which represent the aerodynamic forces and moments, be expressed as coefficients which are functions of as many variables as necessary to account for all aspects of the flight motion under consideration. For example, a pure pitching motion could be represented in a simple form by:

$$(I_{yy})(\ddot{\Phi}) = C_m(\alpha,\beta,p,q,r,M,Rn, \text{ etc.})$$

where I_{yy} is the pitch moment of inertia, $\ddot{\Phi}$ is the pitch acceleration and the total pitching moment is a function of many variables, including angles of attack and sideslip, rotational rates in roll, pitch and yaw, Mach number, Reynolds number, etc. For practicality, the total moment needs to be represented by an approximation consisting of a series of discrete measurable quantities derived by a simple expansion around the various independent variables. For example, one could express C_m in derivative form as:

$$C_m(\alpha,\beta,p,q,r,M,Rn, \text{etc.}) = C_{m_\alpha}\alpha + C_{m_\beta}\beta + C_{m_p}pb/2V + C_{m_q}qc/2V + C_{m_r}rb/2V +$$
$$C_{m_\omega}(\omega b/2V) + C_{m_{\dot\alpha}}(\dot\alpha c/2V) + C_{m_{\dot\beta}}(\dot\beta b/2V) + \text{----------}$$

where the expansion terms are dictated by the ability to evaluate the respective coefficients (derivatives). In most cases the variation in pitching moment due to rotation rates of velocity-vector roll (ω), roll (p) and yaw (r) would be negligible, and therefore the measurement of the pitching moment due to pitch rate (q) and angle of attack change, $\dot\alpha$, would be the only "dynamic derivatives" in pitch that would be important. The cross-coupled terms between pitch and either roll or yaw might be more important at high angles of attack where vortex flows can provide significant influence on the flow field in all axes. If the same equation was written for rolling moment rather than pitching moment (substitute Cl for Cm) different terms would emerge as the most important to keep. It is well known, for example, that there can be substantial cross-coupling effects between roll and yaw at high angles of attack, and so, therefore, one cannot necessarily ignore the occurrence of forces and moments in an axis or plane that is different from the one in which the aircraft is rotating. It becomes even more complicated when one must consider the aerodynamic response to a motion that is a combination of roll, pitch and yaw. Providing wind

tunnel test techniques that can reproduce these combined motions for the purpose of accurately measuring the static and dynamic force and moment inputs is a very difficult proposition. Exploration of combined motion tests is one of the objectives of the present experiments.

Furthermore, it should be noted that the above expressions assume that the pitching moment is only a function of the instantaneous values of the terms in the bracket at the time in question, i.e., it totally ignores motion history effects, which, as stated before, may be of importance under some conditions. The inclusion of these effects, when necessary, further adds to the complexity of the modeling process.

Thus, it is necessary to provide mathematical representations of the aerodynamics in a form that will allow experiments to be conducted to numerically evaluate the terms of the model. The aerodynamic response is then generated on the basis of a "buildup" of a series of coefficients that approximates the "real" free-flight response. Some of the aero-math models, either proposed or in use, are discussed in the next section.

2.3.1 "Traditional" Aero-Math Model

At low angles of attack, where the experimental data acquired from forced-oscillation tests are linear with respect to the rotational rates, the coefficient buildup for the aero-math model is in terms of linear derivatives. For this case, the instantaneous aerodynamic response to motion about the velocity vector can be derived from a simple linear superposition of responses to motion about the body-axis roll and body-axis yaw as shown in the sketch below.

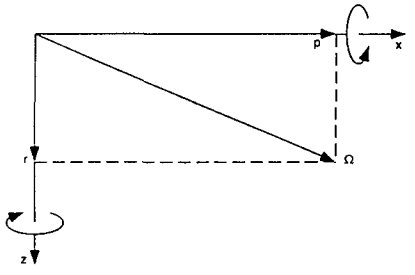

- Used without rotary balance data
- Instantaneous motion is sum of two orthogonal vectors

$$\vec{\Omega} = \vec{p} + \vec{r}$$

$$C_k(\Omega) = C_k(p) + C_k(r)$$

At high angles of attack, however, this approach will not work because the aerodynamic coefficients are nonlinear functions of the rates and the effects of body-axis roll and body-axis yaw motions are not independent.

One approach to partially alleviate this problem is to include rotary-balance test data in the coefficient buildup. These data include the actual combined roll and yaw rate effects where the rotation vector is about the velocity vector. The problem is how to resolve the total rotation vector into components about the three body axes (for the general case) and the velocity vector. There is no unique solution. One approach is to assume that the rotation vector is close to the velocity vector. In this case the total rotation vector is resolved into a component along the velocity vector and a component perpendicular to the velocity vector. The velocity vector component is used with the rotary balance test data and the perpendicular component is resolved back into body axis components and used with the forced oscillation test data. This approach is illustrated in the following sketch.

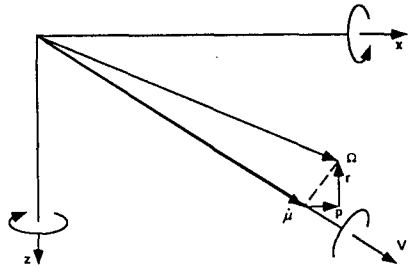

- Used with rotary balance data
- Instantaneous motion is sum of three non-orthogonal vectors

$$\vec{\Omega} = \vec{\dot{\mu}} + \vec{p} + \vec{r}$$

$$C_k(\Omega) = C_k(\dot{\mu}) + C_k(p) + C_k(r)$$

This approach is appropriate for spin motions where the rotation vector is close to the velocity vector. But, in maneuvering flight, the rotation vector can deviate considerably from the velocity vector, so resolving the actual motion primarily into rotation about the velocity vector can lead to significant errors.

2.3.2 Kalviste Model

Another approach was suggested by Kalviste (Ref. 3) This model was derived to allow a better

representation of motions that are dominated by rotation of the aircraft about the velocity vector (so called "loaded roll"), but have oscillatory motions, as well. The basic concept of the model is to resolve the total rotation vector into the three components that are the closest to the total rotation vector instead of the three body-axes components. If the rotation vector is close to the velocity vector, for which rotary-balance data are available, the rotation vector is resolved into three components with one of the components along the velocity vector. In this way the data are always "interpolated" between known data points. The sketch below illustrates the idea with two components in one plane, in this case the velocity vector component (ω) and body-axis roll (p). The third component is either in the x-y plane or the y-z plane (not shown for simplicity).

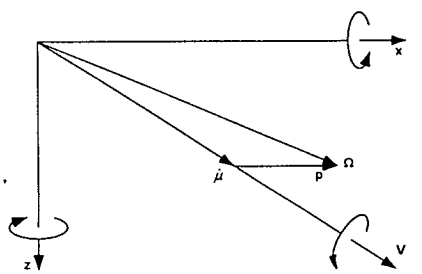

- Used with rotary balance data
- Instantaneous motion is sum of two non-orthogonal vectors

$$\vec{\Omega} = \vec{\dot{\mu}} + \vec{p}$$

$$C_k(\Omega) = C_k(\dot{\mu}) + C_k(p)$$

This approach provides for a unique means of associating all of the motion about the velocity vector with aerodynamic measurements acquired on a rotary-balance apparatus and all of the unsteady or oscillatory motions with the aerodynamic coefficients obtained from small-amplitude forced-oscillation experiments in body axes. This representation is an approximation of the real aerodynamic model, but, for many cases, it is quite effective in providing accurate motion predictions. There are cases where the aero-math model is not sufficient and, therefore, more sophisticated means are required to measure the true aerodynamics.

2.3.3 Improved Kalviste Model

A new approach has been developed (Ref. 2) where the data are interpolated between the actual test data instead of linear combinations of the data (i.e., vector interpolation). This approach is similar to the static aerodynamic data coefficient build-up where the data are interpolated between test data points at different angle of attack an sideslip combinations. The data are interpolated by using test data points on both sides of the point of interest. For the dynamic data the interpolation will be performed between data points (for example, forced oscillation and rotary balance test data) using the total rotation vector magnitude. The interpolation procedure selects the appropriate fraction of the test data coefficients on both sides of the point of interest and sums the two terms. The important point is that the aerodynamic coefficients are being interpolated instead of computing the coefficients with reduced magnitude rotation vectors and then linearly adding the terms. The interpolation is being done by using a newly developed *vector* interpolation procedure (Ref. 2). The vector interpolation is appropriate to use when interpolating between large angles. For example, if data are available for the rotation vector along the x-axis (roll rate) and the z axis (yaw rate), the two vectors are 90° apart. Vector interpolation should be used for any rotation vector between the two axes. If the data are linear with rate then the vector interpolation is equivalent to the conventional procedure of resolving the rotation vector into components along the two axes. For nonlinear data this is not true. Presently, the interpolation scheme has been developed for one-dimensional interpolation for zero sideslip cases, but can be extended to accommodate non-zero sideslip.

2.3.4 Tobak-Schiff Model

In the mid 1970's Tobak and Schiff of NASA Ames proposed mathematical models (Refs. 5-7) which represent a general flight motion in terms of characteristic motions, where the coning motion or velocity-vector roll is one of the primary motions. A general flight motion can be described in terms of body-fixed axes with variables α, β, p, q and r. The resulting formulation, valid for small plunging, and an illustration of the experiments to evaluate the terms are shown in the sketch below. In these equations, the coning rate or velocity-vector roll rate is expressed as ϕ and γ is simply $\cos\alpha\cos\beta$.

$$\hat{C}_k(t) = \hat{C}_k(\infty;\hat{\alpha},\hat{\beta}) + \frac{1}{\gamma}\frac{\dot{\hat{\alpha}}l}{V}\left[\hat{C}_{k_{q_b}}(\infty;\hat{\alpha},\hat{\beta}) + \gamma\hat{C}_{k_{\dot{\hat{\alpha}}}}(\hat{\alpha},\hat{\beta})\right]$$
$$- \frac{1}{\gamma}\frac{\dot{\hat{\beta}}l}{V}\left[\hat{C}_{k_{r_b}}(\infty;\hat{\alpha},\hat{\beta}) - \gamma\hat{C}_{k_{\dot{\hat{\beta}}}}(\hat{\alpha},\hat{\beta})\right]$$
$$+ \frac{1}{\gamma}\frac{p_b l}{V}\hat{C}_{k_{\dot{\phi}}}(\infty;\hat{\alpha},\hat{\beta}); \quad k = \begin{Bmatrix} X, & Y, & Z \\ l, & m, & n \end{Bmatrix}$$

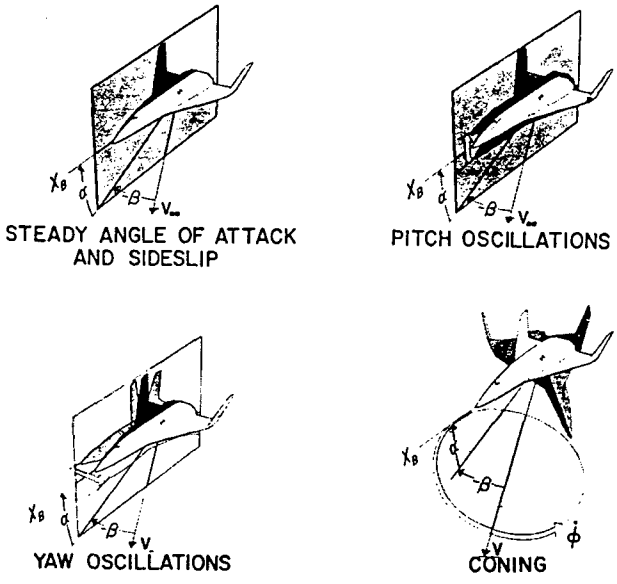

The characteristic motions are: 1) steady planar motion at fixed angles of attack and sideslip, 2) small-amplitude planar oscillations in α with β held fixed, 3) small-amplitude planar oscillations in β with α held fixed and 4) steady coning (velocity vector roll) with both α and β held fixed. For completeness, the measurements of the aerodynamic reactions to the oscillatory motions must include an evaluation of the cross-coupling contributions between the respective axes. In body axes there is no need for oscillations in roll because the roll contribution is contained within the coning motion.

A refinement of this model was derived (Ref. 6) to accommodate a nonlinear variation of the aerodynamic forces and moments with coning rate. The modification makes the model more consistent with wind-tunnel experimental measurements made on aircraft models in coning motion. Three characteristic motions are called for by the formulation in body axes - 1) steady coning motion where the aerodynamic coefficient can vary nonlinearly with coning rate, 2) small amplitude oscillations in pitch in the presence of coning, and 3) small oscillations in yaw in the

presence of coning. The experimental apparatus to perform these combined motions consists of a coning or rotary-balance apparatus where the model is oscillating with small amplitude in either pitch or yaw while being rotated around the velocity vector at different rates. The characteristic motions for this model are illustrated in the sketch below.

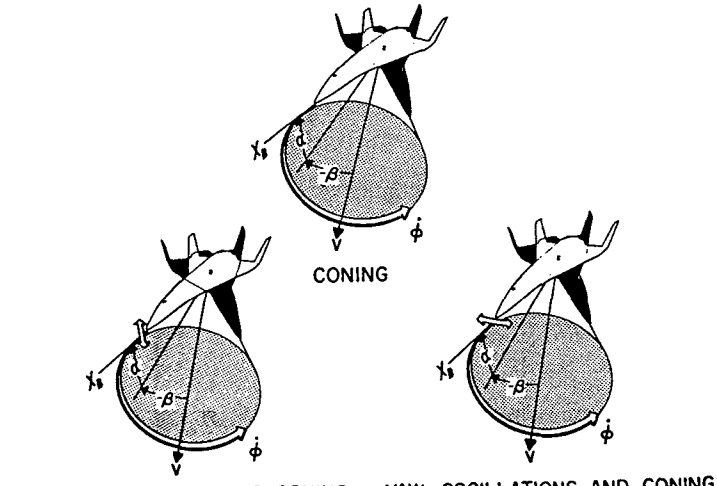

2.3.5 Experiments Consistent with Tobak-Schiff Model - Oscillatory Coning

ONERA-IMFL in France operates a rotary-balance apparatus in a vertical tunnel in Lille where the rotational axis is inclined at various angles to the windstream or velocity vector producing a rotary motion around the velocity vector and, simultaneously, an oscillatory motion with respect to the wind at a frequency equal to the rotational speed of the rotary-balance rig. The amplitude of the induced oscillatory motion with respect to the windstream is determined by the angle of inclination. The following sketches show the apparatus setup, including an illustration of the inclination angle (λ) and the resulting oscillatory variation in angle of attack and sideslip. The results of this experimental approach can be modeled by the Tobak-Schiff model with the restriction that the oscillation frequency cannot be controlled separately from the rotational frequency. However, useful data from combined rotary and oscillatory motion inputs to the model can be obtained. A schematic of the IMFL rig is shown in the sketch below.

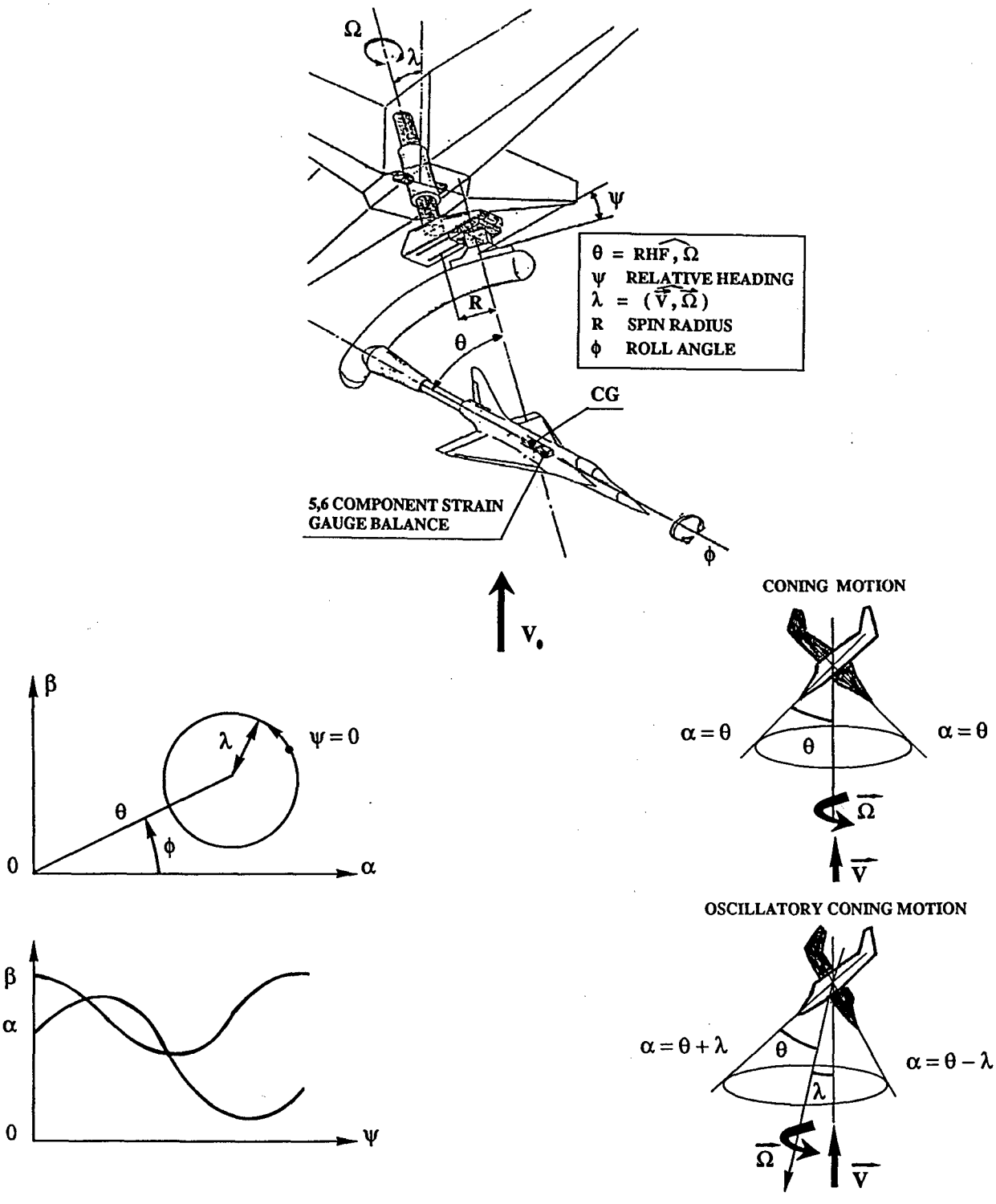

3.0 DYNAMIC TESTING CAPABILITY

There are many facilities which have the capability to perform either small-amplitude forced-oscillation or rotary-balance experiments. Some facilities have the capability to perform both.

AGARD Fluid Dynamics Panel Working Group 11 published a complete document in 1990 on all of the rotary-balance test apparatuses and current test techniques in NATO (and some non-NATO) countries in Ref. 1. Table 1 on the next page is an updated version of a chart from Ref. 1. showing the various rotary-balance test facilities in active use. There are detailed descriptions of these rigs in Ref. 1. AGARD Fluid Dynamics Panel Working Group 16 was organized in response to recommendations from WG 11 to provide follow-up experiments on rotary-balances and forced-oscillation rigs on a common configuration, and, in many cases, on a common model to provide an understanding of the reliability of both rotary-balance and forced-oscillation tests on a fighter-type configuration at high angles of attack. One important objective was to evaluate sting support and facility interference effects on the results. Tests were performed on many rigs in many different tunnels. Table 2, from WG 16's final report, Ref. 8, shows the participating organizations and the test contributions. Each of the rotary-balance and forced-oscillation rigs used in the experiments is described in detail in Ref. 8. Appendix B of this report provides a short description of each of the test rigs/facilities used in the WG 16 experiments and highlights any unusual features or capabilities. For example, while most forced-oscillation apparatuses were designed for small-amplitude oscillations, there are some exceptions which provide high amplitude motions and, in some cases, can provide "ramp" type motions. There are also facilities that can provide rotary-balance and forced-oscillation motions simultaneously, such as the ONERA-IMFL facility described earlier in Section 2.3.

TABLE 1 - ROTARY-BALANCE APPARATUS (REF. 1)

(Representative Values Indicated)

Country	Apparatus Name	Facility	Facility Size	Max Velocity or Mach	Max RN $x10^{-6}/m$	Max Model Span, m	Max Ω rpm	Typical max $\frac{\Omega b}{2V}$	α Range, degrees	β Range, degrees	Model Mass, kg	Inclined Axis Capability	Spin Radius
USA	NASA-Langley Spin Tunnel Rotary Balance	Langley Spin Tunnel	6.7m	30 m/sec	1.8	2.0	90	1.0	-90 to 90	-30 to 30	5	No	Yes
USA	NASA-Ames Rotary Balance	Ames 7 ft x 10 ft Low-Speed Tunnel	2.1m x 3.05m	60 m/sec	3.3	0.7	300	0.2	-60 to 60	-60 to 60	15	No	No
ITALY	AerMacchi 6CR	AerMacchi Low-Speed Wind Tunnel	2m	70 m/sec	3.3	1.3	300	0.3	-180 to 180	-30 to 30	20	No	Yes
UNITED KINGDOM	British Aerospc Low-Speed Rolling Rig	Warton 5.5 m Low-Speed Wind Tunnel	5.5m	22 m/sec	1.5	2.0	60	0.2	0 to 90	-90 to 90	60	No	No
UNITED KINGDOM	British Aerospc Multifacility Derivative Rig	Warton 1.2 m High-Speed Blowdown	1.2m	M = 0.4 to 0.86	30 - 65	0.6	300	0.3	0 to 90	-90 to 90	30	No	No
UNITED KINGDOM	RAE-Bedford Rotary Balance	DRA-Bedford Low-Speed Tunnel	4m x 2.7m	90 m/sec	6.0	0.7	400	0.2	-20 to 60	-60 to 60	15	No	No
GERMANY	DLR Rotary Balance	DLR 3 m Low-Speed Tunnel	3.25m x 2.8m	80 m/sec	5.5	1.0	300	0.3	-30 to 90	-90 to 90	20	No	No
FRANCE	ONERA-IMF Lille Tournebroche Rotary Balance	SV4 Vertical Wind Tunnel	4m	50 m/sec	2.0	1.0	120	0.6	-135 to 135	-90 to 90	10	Yes (20 deg)	Yes
SWEDEN	FFA L2 Rotary Rig	FFA Low-Speed Tunnel L2	2m x 2m	65 m/sec	3.5	0.6	600	0.3	-40 to 40	-40 to 40	5	No	No
SWEDEN	FFA LT1 Rotary Rig	FFA Low-Speed Tunnel LT1	3.6m	70 m/sec	6.0	1.0	360	0.3	-150 to 150	-10 to 10	10	No	No
SWEDEN	FFA S4 Rotary Rig	FFA Transonic-Supersonic Tunnel S4	1m x 1m	M = 0.5 to 2.0	14.0	0.4	600	0.2	0 to 25	0	5	No	No
CHINA	CARDC Rotary Balance	CARDC 4m x 3m Low-Speed Tunnel	4m x 3m	100 m/sec	6.0	1.0	330	0.2	-135 to 135	-45 to 45	15	No	No
CHINA	Chinese Aero-nautics Estab. HARI RB-1	FL-8 Low-Speed Tunnel	3.5m x 2.5m	N/A	N/A	N/A	300	0.2	-126 to 126	-36 to +36	N/A	Yes	No
USA	WPAFB Rotary Balance	Wright Labs Spin Tunnel	3.7m dia.	50m/sec	3.4	1.2m	130	0.6	-90 to +90	-30 to +30	12	No	No
GERMANY	BAR Rotary Balance	Large Amplitude Multi-Purpose Facility	3.3m dia.	40m/sec	2.0	1.0	150	0.5	-180 to +180	±32	10	No	Yes

TABLE 2 - PARTICIPANTS IN AGARD WG 16 EXPERIMENTS

Organisation	Type of test
AerMacchi (AEM), Italy	Rotary
Defence Research Agency (DRA), United Kingdom	Rotary & Oscillatory
Deutsche Forschungsanstalt für Luft und Raumfahrt (DLR), Germany	Rotary
Eidetics Corporation/NASA Ames (EI), USA	Rotary
Institute for Aerospace Research, (IAR), Canada	Oscillatory
Institut de Mécanique des Fluides de Lille (ONERA-IMFL), France	Rotary & Oscillatory
Politecnico di Torino (TPI), Italy	Oscillatory
Flygtekniska Försöksanstalten (FFA), Sweden	Rotary
NASA Langley/Bihrle Applied Research/DRA	Rotary (pressure measurements)

4.0 AERO-MATH MODELS AND EXPERIMENTS - SHORTFALLS

4.1 Nonlinear Effects

As discussed previously, for the high-angle-of-attack regime, most, if not all of the aerodynamic coefficients vary non-linearly with rotation rate so expressing the aerodynamic coefficients in derivative form over the entire angle of attack range can lead to significant errors in representing the aerodynamics properly. The compromise approach to date has, in many cases, resulted in nonlinear data being acquired from rotary-balance data (coefficients often show highly nonlinear variations with rotation rate) and from small-amplitude forced-oscillation experiments which assume that the airframe data varies linearly with increasing/decreasing oscillation frequency (rate). For many configurations and flight regimes, this assumption of linearity with rotational rate is grossly inappropriate and can lead to serious errors in representing actual motion behavior. For some configurations, this combination is satisfactory because most of the nonlinearity is in the motion around the velocity vector and the motion around the body axes are close enough to linear with body rates to be acceptable. For motions with large-amplitude rotational excursions in body axes this means of representing the aerodynamic model would not be accurate.

4.2 Superposition

Because many of the aerodynamic responses to motion are nonlinear in character, it is also a problem to superpose results from different axes. Most test results generated from different data sets are nonlinear in nature and a composite representation cannot be found simply by linear superposition of results from different tests. Therefore, it is important to devise an improved means of properly combining test data from different experiments to represent the actual motion in free flight.

4.3 Time-History Effects

As already mentioned, motion history effects can become very important under some conditions. In these cases the locally linear aerodynamic model fails, rendering the representation of airloads in terms of instantaneous attitude and rate ineffective for prediction purposes, as the actual value of the loads is also highly dependent on the motion history leading up to the instant in question. This can be clearly inferred from the significant differences in experimental results obtained for a given attitude and angular rate as a function of oscillation frequency or amplitude or from a continuous motion. The length of time over which the motion history is relevant can be many convection times, depending on the response time of the physical phenomena responsible for the motion history effect. The data obtained from small amplitude oscillatory tests cannot, therefore, be used to "build up" results for large amplitude motions. The actual motion history of interest must be created with real-time measurements of the aerodynamic response.

5.0 ADVANCED EXPERIMENTS FOR NONLINEAR MEASUREMENTS

5.1 Institute for Aerospace Research/Wright Lab Experiments on a Delta Wing

In order to address the important modeling issues raised above, the Institute for Aerospace Research (IAR) and Wright Laboratory (WL) undertook a joint program in the late 1980s to explore the aerodynamic behavior of vehicles during high-performance maneuvers involving large-amplitude high-rate motions at high angles of attack (Refs. 9-11). The main thrust of the program was to gain a clearer understanding of the reasons that caused existing aerodynamic models to rather poorly represent the aerodynamics present under advanced maneuvering conditions and hopefully develop more appropriate modeling methods. Much of the emphasis was placed in better grasping the flow physics present in that regime as it was expected that therein was the key to the

problem. Some of the more important findings of the program have been incorporated elsewhere in this report, so only some of the more salient experimental results leading up to those conclusions are described here.

Special roll and pitch wind-tunnel rigs were developed to allow imparting motions of realistic amplitude and angular rates to the model, as these were deemed to be necessary to elicit the non-linear and unsteady effects present under actual maneuvering conditions, something small-amplitude low-rate rigs could not properly do. Rolling experiments conducted on a 65° delta wing model yielded extremely interesting results that demonstrated the inadequacy of the locally linear model and some of the main causes underlying it.

The static rolling moment coefficient as a function of roll angle for a sting angle (σ) = 30° and 35° are shown in Fig. 1.

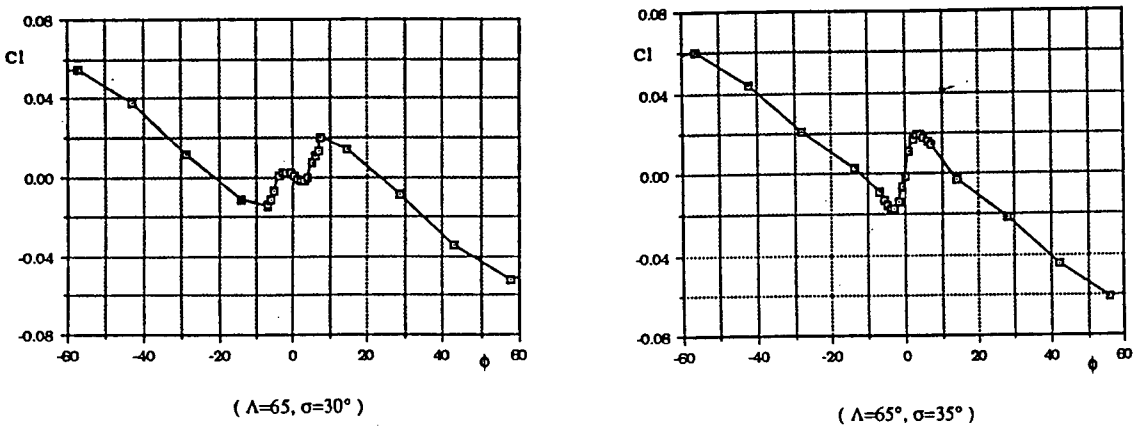

Figure 1 - Rolling moment coefficient

All results were obtained for M~0.3 and Re=2.4 million. The very non linear areas around the origin are caused by the presence of leading-edge vortex breakdown over the wing. There are 3 and 2 stable roll trim points (roll attractors) respectively for the cases shown. It can be seen that for the case of σ=30° the attractor basin for the attractors at ϕ=±21° is far larger than that for ϕ=0°, suggesting that in free-to-roll experiments, possible to perform with the roll rig, the model would only trim at 0° if released from a very small roll angle. Motion histories for two releases with σ =

30° are shown below together with predictions based on a locally linearized model, where the total moment was calculated based on the local value of the static moment (not static derivative times deflection) plus a damping term based on local damping derivatives obtained from 5° amplitude oscillatory tests.

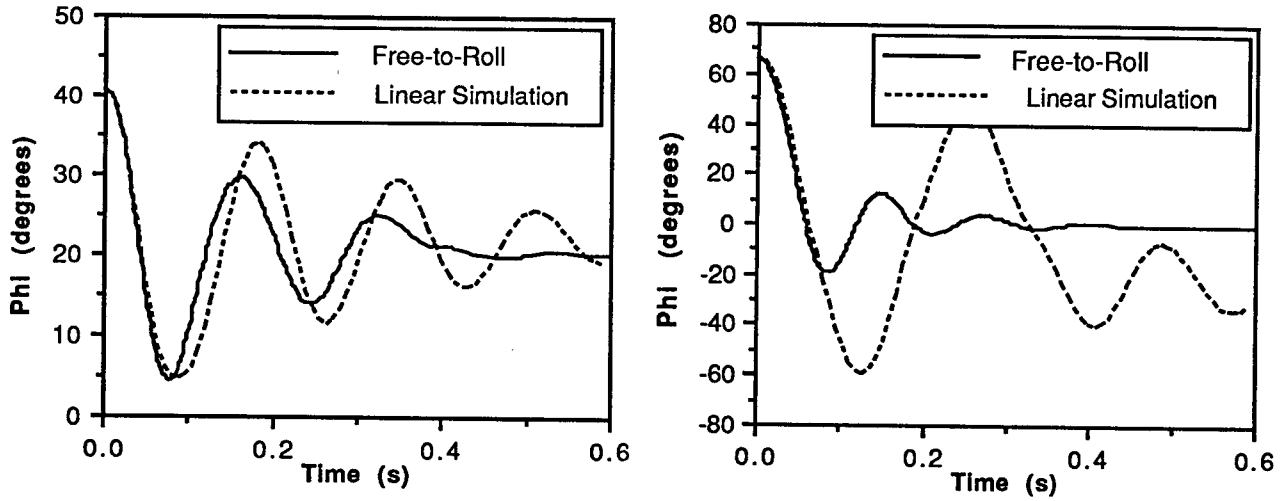

Figure 2 - Motion time histories for releases at ϕ=41° and ϕ=66° with σ = 30°

In the first case the model, after being released from ϕ_i = 41°, trims as predicted by the locally linear model, although the damping is considerably underestimated. In the second case the model was released from ϕ=66°, stopping after the first half cycle at ϕ = -21° where a roll attractor is located, but rather than remaining there, the motion continues in an oscillatory fashion until it settles down at the 0° trim point. In this case the locally linear model utterly fails to predict not only the overall motion but even the trim point!

A phase plane representation of three free-to-roll motion histories, superimposed to the phase portrait based on the locally linear model is shown in Fig. 3. The intersections between trajectories are due to the fact that the moment is not only a function of roll angle and rate, as required by the locally linear model, but is also determined by other unaccounted for effects. Moreover the crossings of separatrices corroborates that the model is totally incapable of representing these effects following critical-state encounters. These results have been qualitatively explained in terms of vortex breakdown, which being characterized by very slow propagation speeds (almost one order of magnitude slower than freestream velocity) clearly point out the importance of motion history effects.

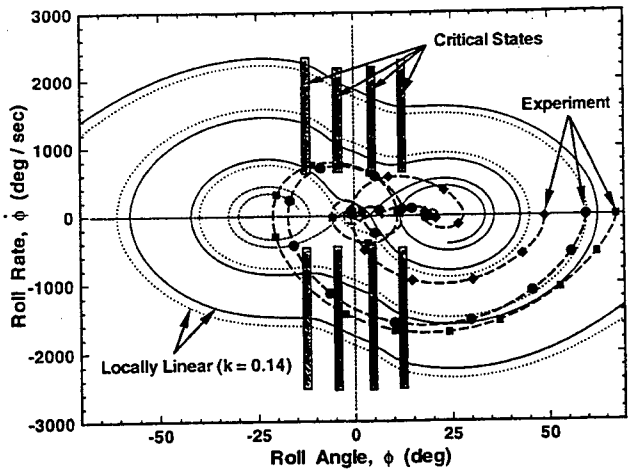

Figure 3 - Actual free-to-roll motions vs locally linear phase portrait

To further examine the limitations of locally linear derivatives, data from forced oscillation experiments were reduced as in the free-to-roll simulations, i.e., the non-linear static rolling moment data were used together with the roll damping derivatives obtained from 5° amplitude tests. Only the quadrature component at the rolling frequency was retained, although up to 20 harmonics were recorded. Thus the result is a derivative about the mean angle of the motion. The locally linear model was then used to "predict" the measured rolling moment over the same motion as used to determine the damping derivative. Comparisons between the predicted and measured responses for an offset roll angle of 3° and two reduced frequencies are shown in Fig. 4.

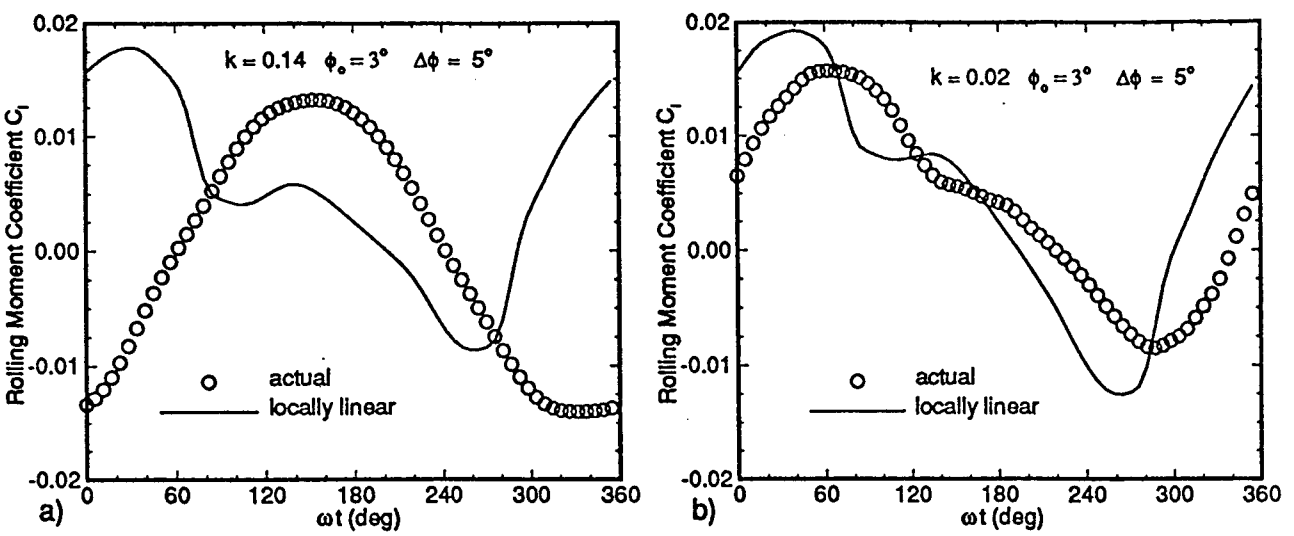

Figure 4 - Comparison of predicted and measured roll responses for an offset roll angle of 3° at k=0.14 and 0.02

The prediction for k=0.14 is totally unacceptable as over most of the cycle even its sign is the opposite to the observed one. At k=0.02 the agreement is better due to the smaller dynamic effects present, yet the prediction fails to capture the delay present in the measured moment. These observations demonstrate that even under small amplitude motions, the locally linearized model may fail to reflect the actual loads, which in this case occurs because of the presence of breakdown over part of the oscillation cycle. Clearly, if such errors can occur when applied to the motion that generated the damping derivative, it can be expected, and it has been demonstrated, that extrapolating the damping component in terms of amplitude or rate can make matters considerably worse.

It should be noted that the unsteady effects introduced by vortex breakdown are not only observed at moderate to high reduced angular rates but even at extremely low ones as shown in Fig. 5, where transient ramp motion results are depicted together with static ones for $\sigma = 30°$.

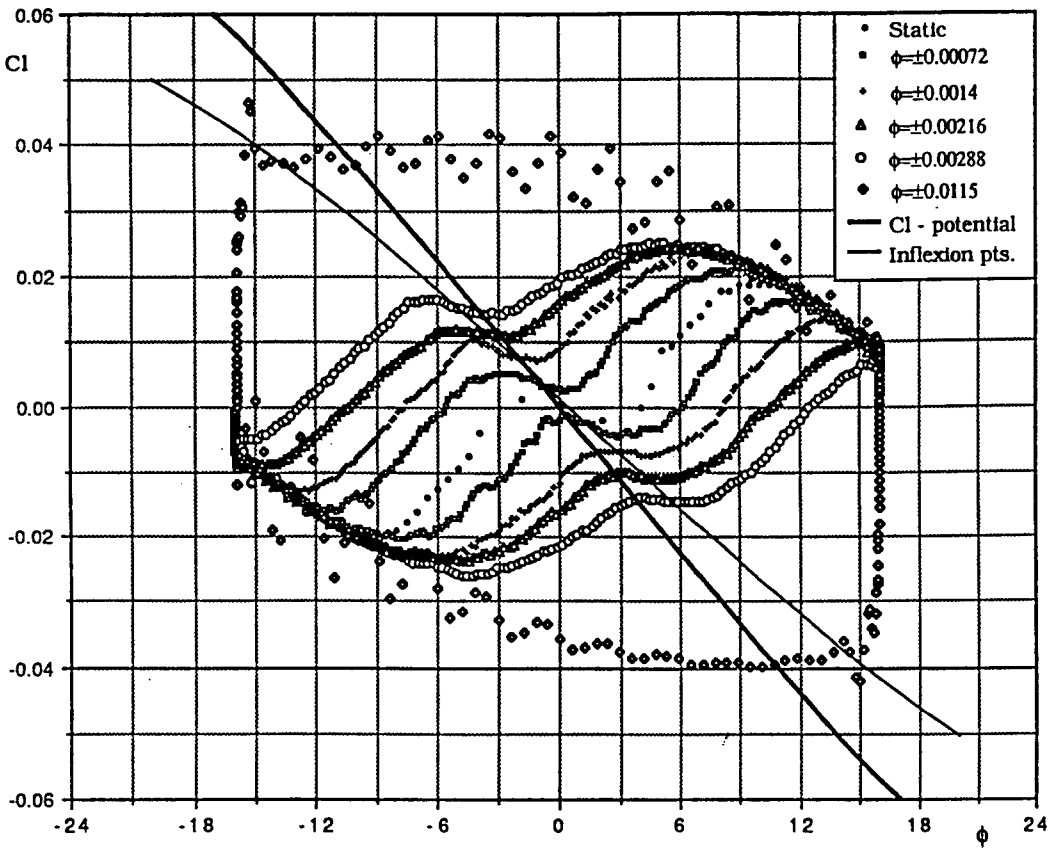

Figure 5 - Rolling moment undergoing ramp roll motions ($\sigma = 30°$)

The model was rolled between $\phi = \pm 16°$ at a constant angular rate and sufficient dwell time was provided between transitions to allow for a complete flow relaxation. The oscillatory component of the rolling moment at the highest angular rate is of inertial origin, apparently resulting from minute servo-system-induced oscillations about the desired instantaneous position. The dynamic loads agree closely with the static ones for $16° > |\phi| > 12°$ at the beginning of the motion, at which point the vortex breakdown on the windward wing begins to move aft from the apex (defining a critical state). Once the critical state is encountered the dynamic loads overshoot the static values by increasing amounts depending on the angular rate. As can be observed, even for $\dot{\Phi} < 0.001$ a very distinct overshoot is present which persists for most of the motion. As expected, the higher the rate the later (in terms of roll angle) the dynamic results coalesce with the static ones. In fact at the two highest rates this occurs during the dwell time after the completion of the ramp motion. It should be noted that the observed transient in the dynamic load is typical following an encounter with a critical state and cannot be captured by locally linear aero models.

Several approaches are being explored to improve models applicable to the advanced maneuvering regime. The reaction hypersurface model developed by Hanff (Ref. 12) is based on the description of the instantaneous value of the aerodynamic reactions in terms of the corresponding values of the motion variables and their time derivatives. In a topological sense each airload can thus be defined by a multi-dimensional surface that describes it as a function of these variables and time derivatives. The instantaneous value of the airloads are stored in look-up tables as functions of the motion variables and their derivatives and can be used as forcing functions in the equations of motion in order to perform simulations. Motion history effects can in principle be accounted for by using higher order time derivatives of the motion variables, however practical limitations generally impede the use of higher than second order derivatives. As a result, "long past" history effects are difficult to model, although this problem can be mitigated by a judicious selection of motions with which to populate the phase hyper-space, which is generally done with realistic amplitude and rate motions, made possible by the use of the high-performance rigs specially developed for this purpose. Predictions of free-to-roll motions using the Reaction Hypersurface model yielded much closer results to experimentally observed ones than those based on the locally linear model.

Jenkins and Hanff demonstrated that the reaction hypersurface model is a sub-set of the non-linear indicial response approach proposed by Tobak, and have been working to find ways to utilize the latter in a practical sense for flight mechanics predictions. The substantial mathematical complexity of the problem renders this effort very difficult, but significant progress has been made. The

analytical work has partly relied on wind-tunnel experiments tailored to the requirements of the non-linear indicial response method utilizing the above mentioned high-performance rigs.

Given the pivotal role that vortex breakdown plays in determining the airloads, precisely in the areas where the locally linear model breaks down, Huang and Hanff are developing a model based on prediction of the instantaneous vortex breakdown locations on delta wings, which is then used in combination with an unsteady surface pressure model that incorporates the effect of breakdown, to predict the airloads. This approach has yielded good normal force predictions under a large number of conditions. However good moment coefficient predictions have proven to be more elusive to achieve as they heavily depend on the accuracy of the assumed spanwise and chordwise surface pressure distribution. Work to improve the unsteady surface pressure model is continuing.

The above researches believe that to effectively model airloads it is necessary to have a certain understanding of the flow physics which in turn requires a specific testing methodology. Of particular importance is having knowledge of the presence of breakdown and more generally of the existence of critical states as they may introduce dramatic departures from a locally linear aerodynamic behavior during a maneuver. Detailed static force/moment tests can be used to find critical states which are recognizable by discontinuities in the airloads or their slopes to and on/off surface flow visualization tests, which must then be complemented by suitable dynamic tests.

6.0 PROPOSED PHASE I EXPERIMENTS

The Phase I experimental work was originally planned to focus on determining which dynamic aerodynamic coefficients are the most relevant for evaluating the flight characteristics of modern fighter and transport aircraft and to determine the most effective method for modeling and measuring these dynamic coefficients. The measurement of the relevant dynamic coefficients was intended to be accomplished with a unique method of dynamic testing in the Eidetics' water tunnel using a sophisticated 3-axis computer-controlled model support and a high-sensitivity force and moment balance. The approach was based on previously demonstrated success in conducting dynamic experiments in the water tunnel where 5 components of forces and moments (no axial) were measured on a model undergoing computer-controlled large-amplitude motions in either pitch, yaw or roll. Because of the low free stream velocity of the water tunnel, the required model motion rates are quite low, and acquisition of force and moment responses to the commanded motions was relatively straightforward. This experimental test capability is not limited to the assumptions of linear aerodynamics with respect to rotation and/or translation rates, as is the case for low-amplitude forced-oscillation experiments.

In addition to performing large-amplitude oscillations and ramp-type motions in a single axis (pitch, yaw or roll), the plan was to explore some examples of acquiring data with the model undergoing simultaneous motions in 2 axes. The model used for most of the experiments was a 1/48th-scale F/A-18 because of the already existing data base from wind tunnel tests and from previous experiments in Eidetics water tunnel. It also is an appropriate configuration to use because of the specific interest from the Navy, the sponsor of the Phase I work. An added advantage is the capability of the water tunnel to provide flow visualization simultaneously with the measurement of forces and moments.

6.1 Advantages of Water Tunnel Tests

One of the difficulties in producing motions with models in the wind tunnel is obtaining the required rotational rates that must be achieved because of the high tunnel air speeds. The rotation rate scaling parameter, sometimes referred to as the reduced frequency or non-dimensional rotation rate, is $\omega b/2V$, where ω is the rotation rate, b is the reference wing span and V is the free stream velocity. The free stream speed of the water tunnel, consistent with good flow visualization and adequate for force measurements in the Eidetics water tunnel with a high-sensitivity force and moment balance, is typically 1 ft/sec or less, at least a factor of a hundred less than a typical low-speed wind tunnel. The benefit to dynamic testing in the water tunnel is that the requirement for rotation rates are also on the order of a hundred less than rotation rates required for a wind tunnel. This makes it possible to do dynamic tests in the water tunnel with rotational motions about pitch, yaw and roll axes at rates typically less than 10 /sec. Table 3 shows the relative motion requirements for flight, wind tunnel and water tunnel tests in order to provide the same reduced or non-dimensional rotation rate.

	FULL SCALE AIRCRAFT	WIND TUNNEL ROTARY TEST	WATER TUNNEL ROTARY TEST
$k = \frac{\omega b}{2V}$	0.2	0.2	0.2
V	300 fps	200 fps	8 ips
b	40 ft	2.4 ft	10 in
ω	170 deg/s	1900 deg/s	18 deg/s

Table 3 - Rate scaling from sub-scale to full-scale

Previous large-amplitude dynamic experiments on an F/A-18 model in the Eidetics water tunnel are described in Refs. 12 and 13. These experiments consisted of both rotary-balance experiments and large-amplitude oscillatory and ramp motions in pitch, yaw and roll. A schematic of the Eidetics water tunnel is shown in Fig. 6

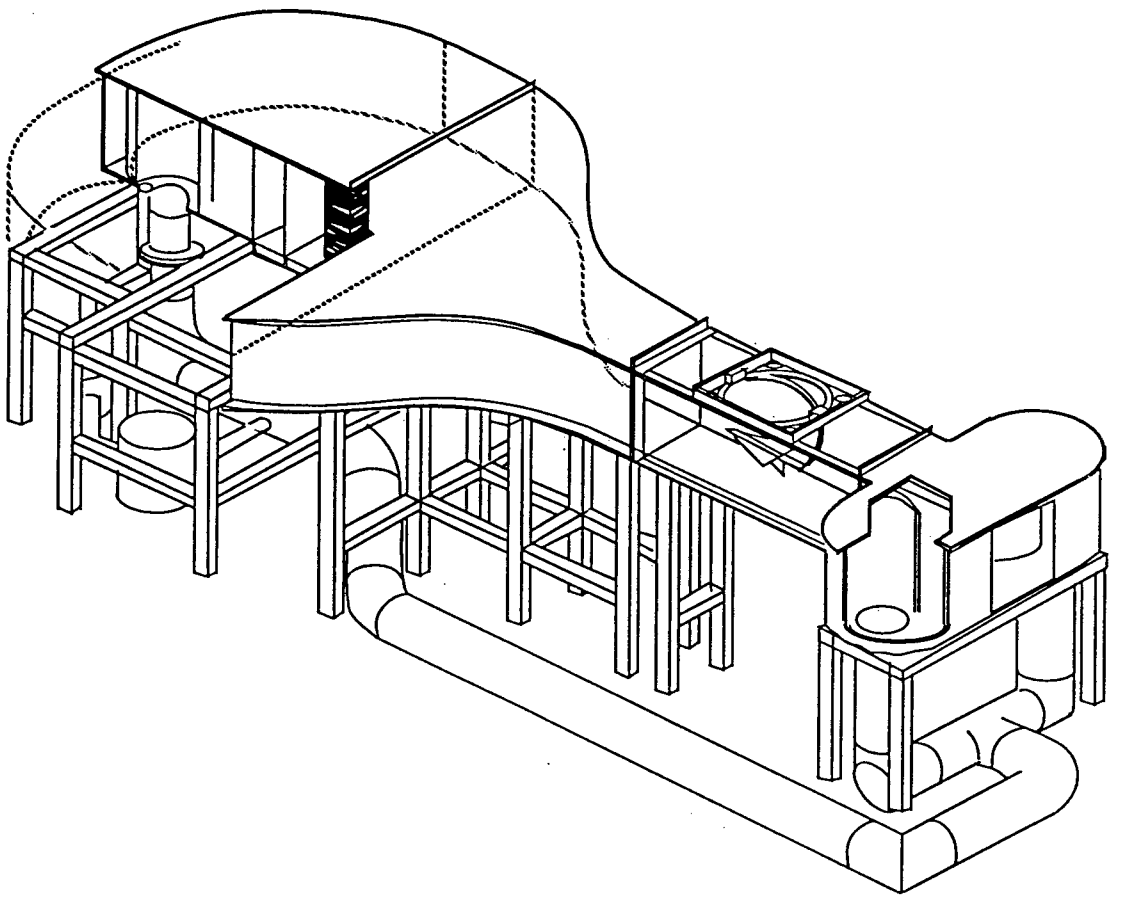

Figure 6 - Schematic/Photo of Eidetics Water Tunnel

Some examples of these experiments are shown in Figs. 7-10. Figure 7 (Ref. 13) shows an example of the lag in the pitching moment with a pitch-up and a pitch-down maneuver between the angles of attack of 15 and 65 . The effects on the level of pitching moment compared to static data are significant for both pitch up and pitch down and are highly dependent on the pitch rate.

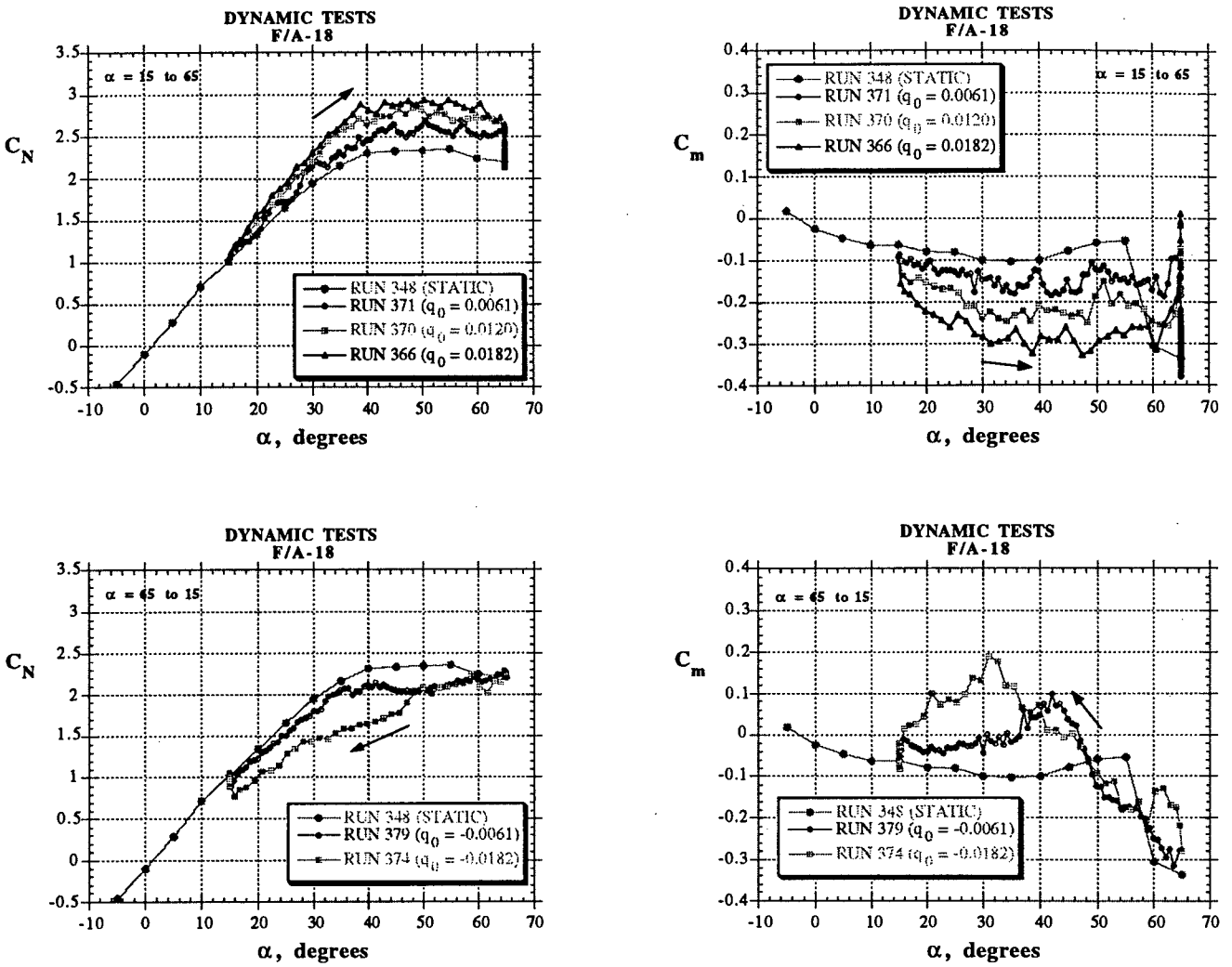

Figure 7 - Effect of Pitch Rate on the Longitudinal Characteristics of the F/A-18

Another example is the hysteresis effects in an oscillatory yaw motion, shown in Fig. 8 (Ref. 3). Rolling moment coefficient and sideslip angle time histories are shown in Fig. 8a for the F/A-18 at 30 angle of attack at 2 different frequencies. The hysteresis loops in rolling moment with sideslip at both frequencies are shown clearly in Fig. 8b. Similar experiments were conducted in roll with clear definitions of the hysteresis effects.

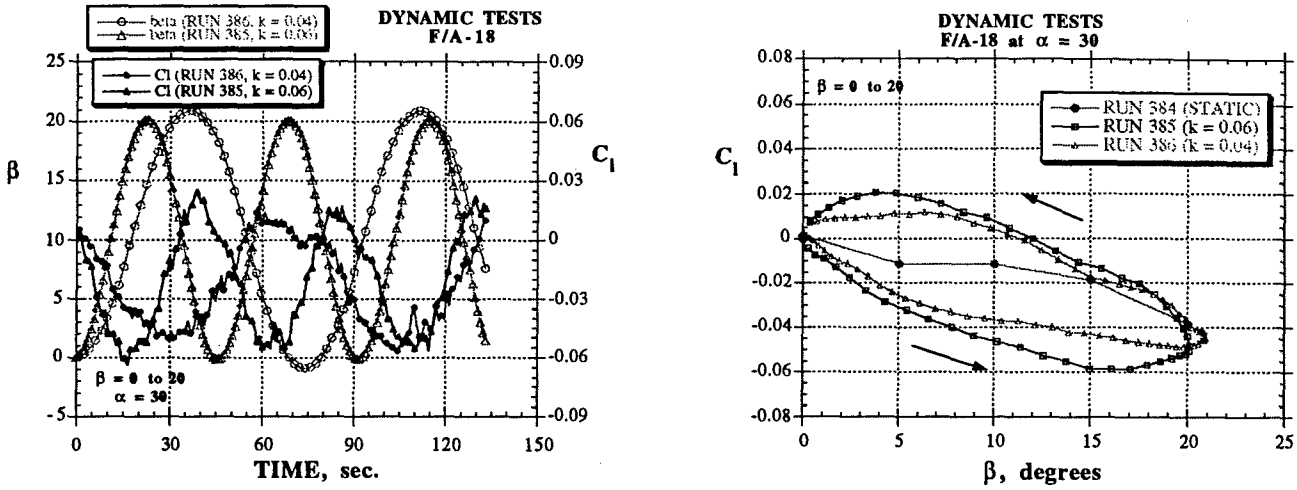

Figure 8 - Results of Dynamic Yaw Oscillations (1/48th-Scale F/A-18 Model at $\alpha = 30$)

Rotary-balance experiments were also conducted on the same model with the rig shown in Fig. 9 (Ref. 3).

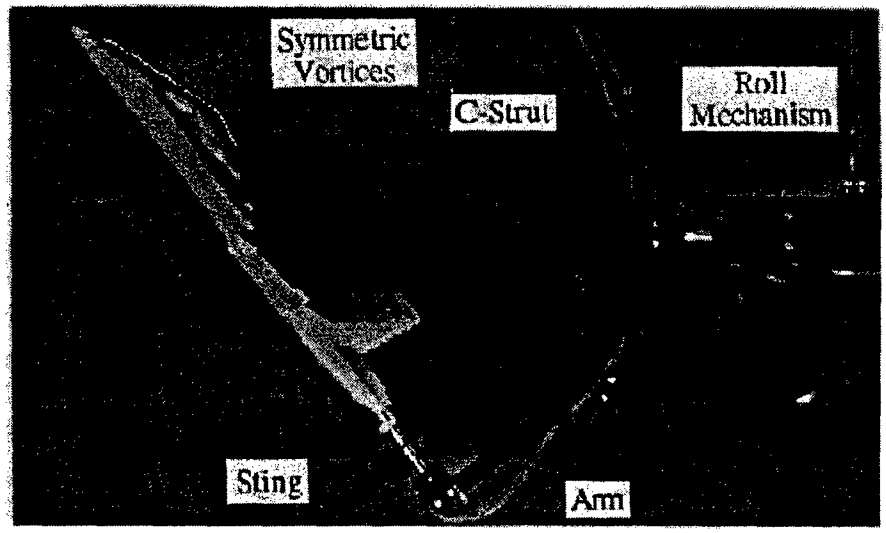

Figure 9 - 1/48th-Scale F/A-18 Model on water tunnel rotary-balance rig at $\alpha = 50$

The yawing and rolling moments at 50 angle of attack are shown in Fig. 10 (Ref. 14) with a comparison to wind tunnel data (Refs. 15 and 16). The trends are very similar, as was demonstrated with the other coefficients.

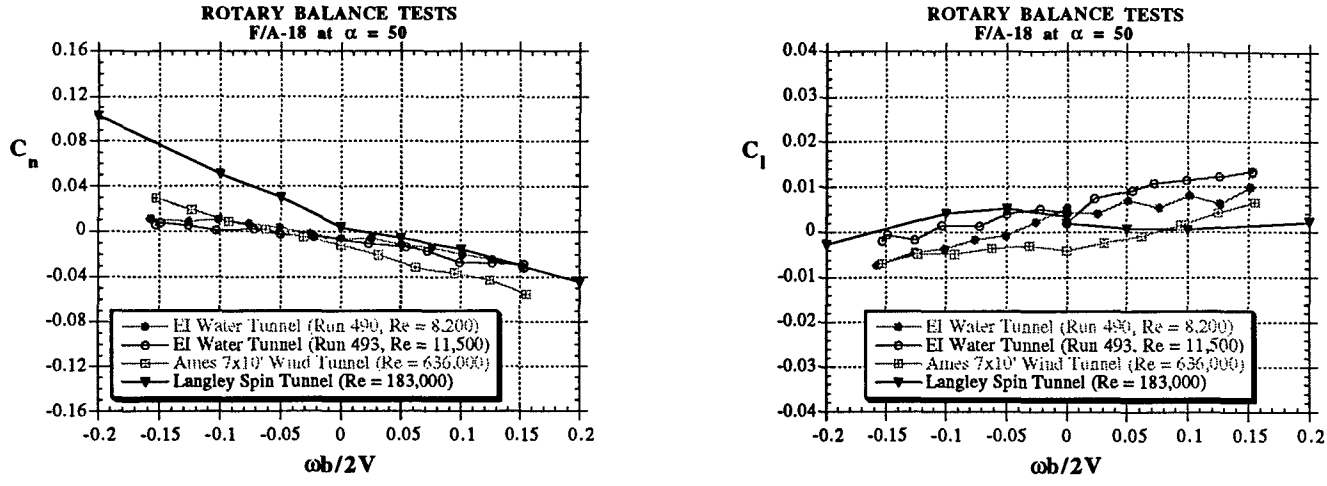

Figure 10 - Results of water tunnel rotary balance experiments on the F/A-18 Model at $\alpha = 50$

In principle the complete test capability in the water tunnel provides a means of acquiring data in all modes of motion, ranging from small amplitude oscillations in one plane to large amplitude motions in more than one axis. The attractiveness of this approach is that all of the experiments can be done with the identical model at identical test conditions. This provides a self-consistency for the data base that should eliminate any questions about effects of model support, test conditions, facility differences, etc.

With this background success in observing and measuring dynamic effects the Phase I experimental effort was directed towards demonstrating the feasibility of using the water tunnel for acquiring dynamic data over a wide range of motion conditions from simple forced-oscillation motions (small- and large-amplitude) and ramp-type motions around individual body axes and both oscillatory and continuous rolling motions around the velocity vector and various combinations of the above motions. The results of these exploratory experiments and the problems encountered in the performance of the tests, particularly those associated with the quality of the balance output signal and data acquisition and reduction challenges with low signal-to-noise ratios are discussed in the next section. The discovery of some of these data acquisitions difficulties has revealed that the model support drive system and accurate acquisition of data (particularly small-amplitude and high-rate motions) are prime targets for improvements in a Phase II effort in order to be able to measure the dynamic aerodynamic terms over a wide range of conditions with sufficient accuracy to be useful.

7.0 PHASE I EXPERIMENTAL RESULTS

7.1 Objectives of Experimental Investigation

The utility of the water tunnel for investigating flow physics, especially vortex behavior, through flow visualization has been well established. The new ability to perform force and moment measurements has not had such a long history. Apart from the ability to obtain unsurpassed flow visualization and the attending insight into the fundamental flow physics, use of the water tunnel for dynamic experiments offers unique advantages.

The recently developed, sensitive, submersible internal balance allows testing at very low freestream velocities. The effect of a low freestream velocity on the scaled angular rates has been mentioned previously in this report, but there are additional benefits to the low speed. The whole motion control challenge is reduced to such an extent that it is possible to perform almost any arbitrary motion desired. No longer is the investigator constrained to sinusoidal motions. Data acquisition rates are likewise reduced. In spite of using a fairly dense working fluid in the test section, the dynamic pressures are small enough that lightweight, simple models can be used. Due to the similarity in the average density of the model structure and the working fluid, inertial effects of motion accelerations are reduced to the point where they could be safely ignored if desired. This adds to the ease of extracting data from arbitrary motions since inertial tares do not need to be accounted for[1].

Drawbacks of using a water tunnel stem from the small scale of the models, causing difficulty in maintaining geometric similarity and contributing to a very small Reynolds number. Previous experiments established that the water tunnel could reproduce the static and dynamic test capability of wind tunnel experiments, at least for the few configurations investigated. The primary objective of the current experiments was to determine if the water tunnel would be a useful tool for investigating some of the more troublesome questions regarding non-linear dynamic aerodynamic modeling that are beyond the ability of wind tunnels to test. If that potential was established, then the experiments would attempt to begin the investigations of non-linear dynamic aerodynamics.

---

[1] Note that the data reduction technique used for this work, does, in fact, remove inertial effects in addition to gravity, buoyancy, and apparent mass effects.

7.2 Limitations of current water tunnel system

A problem established itself immediately upon beginning the investigation. The water tunnel model support structure was originally designed with only static tests in mind and, as a result, the support hardware is somewhat too flexible for the time varying forces of dynamic testing. Likewise, the data acquisition system was designed for steady-state testing and needed some modifications to permit the higher data rates required during properly scaled unsteady maneuvers. These limitations are recognized and the necessary improvements required to refine the system are well understood. Upgrades to the model support and data acquisition systems are proposed as the first task before further research.

Limitations in the current set-up were not expected to seriously impact the primary objective, that is, to determine the viability of the water tunnel to investigate non-linear dynamic aerodynamics. The limitations, however, will adversely effect the ability to draw conclusions from the investigation of non-linear aerodynamic modeling.

7.3 Discussion of Experimental Investigation

It has been demonstrated many times that during maneuvering flight, the aerodynamic reactions can become non-linear with angles and rates, time history dependent, with lags, overshoots, and hysteresis effects.

Exploration of basic nonlinearity of the aerodynamics was not addressed directly. Instead, two issues of fundamental importance to the issue of aerodynamic modeling were explored. These issues are the effects of motion time history and the applicability of superposition.

Effects of motion time history will be investigated through a series of roll oscillations of varying amplitude and rate. This series of tests will attempt to span between the small amplitude forced oscillation technique and the continuous rotary balance technique. In common wind tunnel practice, these two classes of tests are performed in different facilities with different models – not surprisingly they yield different answers. Unanswered questions are: how small an oscillation is too small, and why do the two techniques give different results. Additionally, some insight is expected into possible effects of the developing wake.

The assumption of superposition manifests itself throughout aerodynamic model build-up methods and experimental test techniques. There are a number of schemes for decomposing an arbitrary motion into component parts for which the aerodynamic contribution of each are known. Some of the more common will be investigated. The ease of motion control in the water tunnel allows not only aerodynamic measurement during the single axis component motions, but also during complex multi-axis motions, thereby allowing the various superposition schemes to be tested and verified.

7.3.1 Roll Amplitude Effects

Symmetric triangular waveforms are used so that there will be a period of constant rotational velocity where the rate effects can be determined. An array of amplitudes and rates was tested as shown in the following table.

Rates	**Amplitudes**			
4°/s	±5°	±10°	±15°	
8°/s		±10°	±15°	
12°/s			±15°	±30°

It was not feasible to test smaller amplitudes due to the abrupt direction reversals causing "ringing" of the model support which degraded the quality of the data.

The measured rolling moment coefficients are shown plotted against the roll angle. Figures 11-13 show three amplitudes at the slowest roll rate, 4°/s. The vertical distance between the upper and lower portions of the loops is an indication of the effect of roll rate on the roll moment, i.e., the amount of roll damping. The direction of travel around the loops is counterclockwise, and shows that for negative roll rates (the upper loop), the total roll moment is positive, meaning the aerodynamics resist the motion. Also shown on the plot are static roll moment measurements over the roll angle range. As can be clearly seen from Figures 12 and 13 the damping increment is not symmetric about the static curve. In fact, when the magnitude of roll is increasing, the resistive contribution due to the motion disappears, suggesting a possible instability.

Inspection of the three plots shows that the damping is fairly consistent over the entire range of oscillation. The absence of an amplitude effect might imply that the wake formation does not play a significant role at these slow rotation rates.

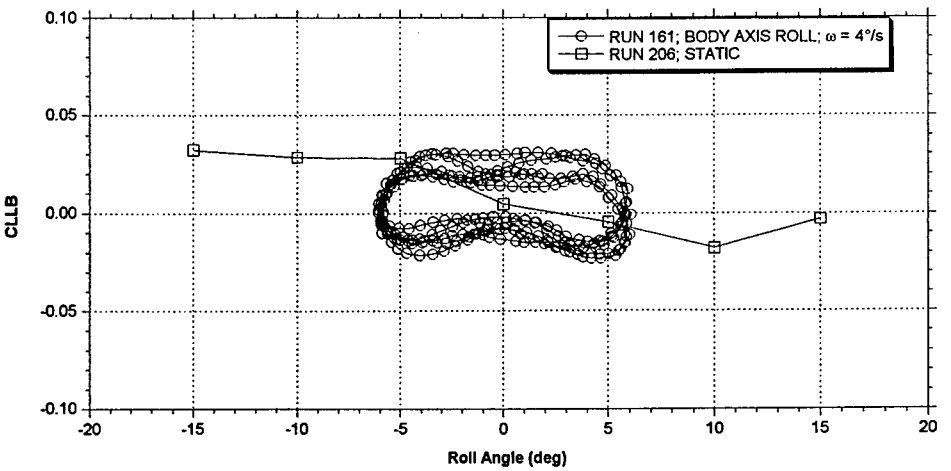

Figure 11 - F/A-18 (1/48 scale) Body Axis Roll Oscillation

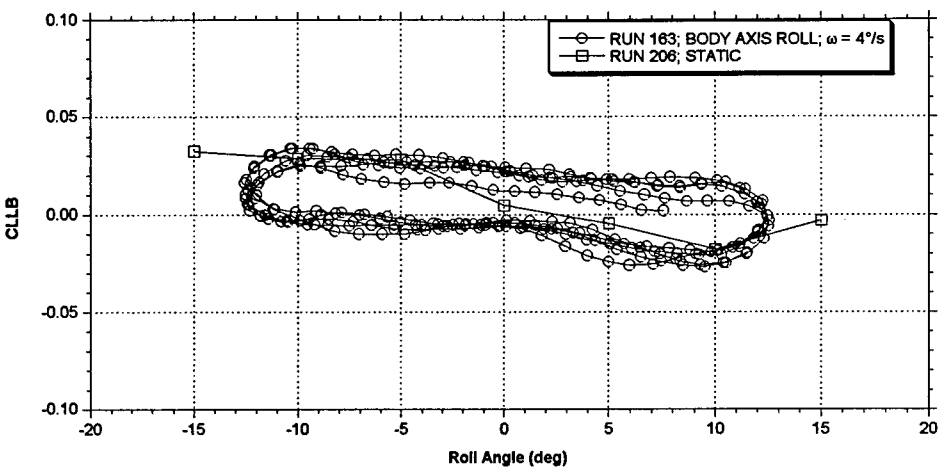

Figure 12 - F/A-18 (1/48 scale) Body Axis Roll Oscillation

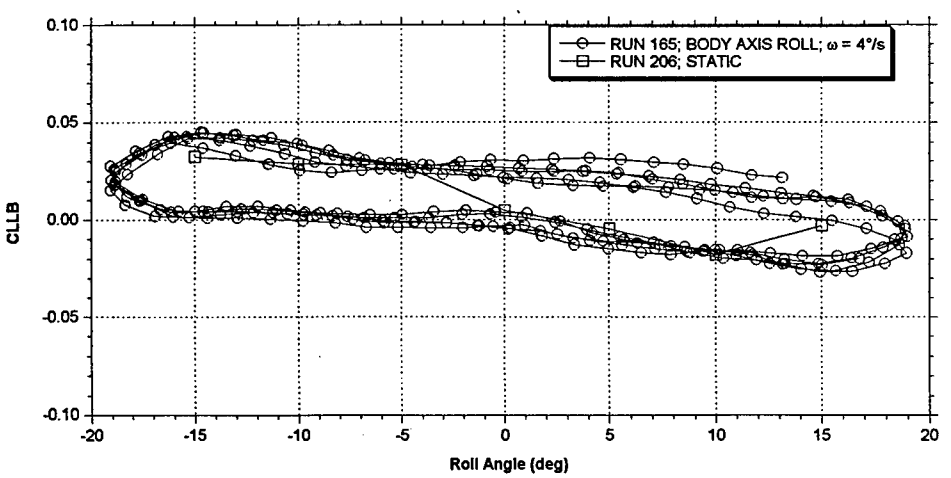

Figure 13 - F/A-18 (1/48 scale) Body Axis Roll Oscillation

Figures 14 and 15 show repeat oscillations at the larger amplitudes but with twice the angular rate. Again, the distance between the upper and lower loops is fairly uniform and is about twice that seen in at half the rate in the previous set of figures. At this higher rate, damping is present during increasing magnitude motions but at a lower level than when the magnitude is decreasing.

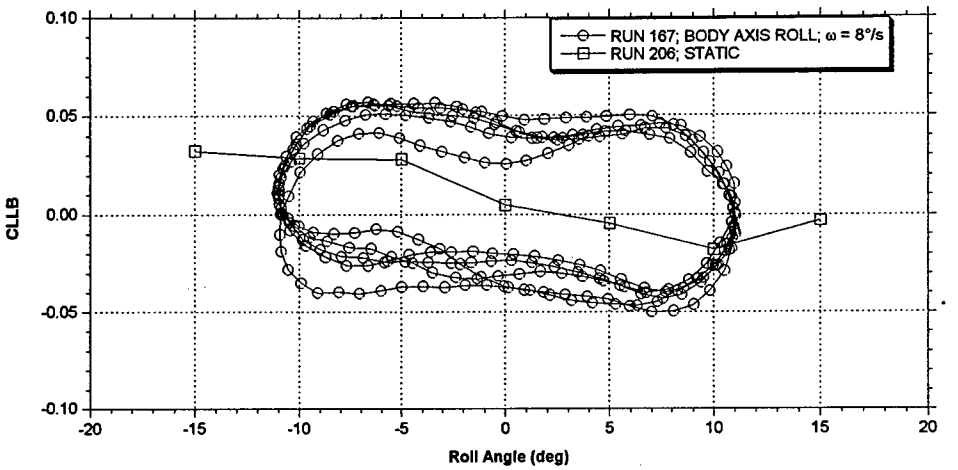

Figure 14 - F/A-18 (1/48 scale) Body Axis Roll Oscillation

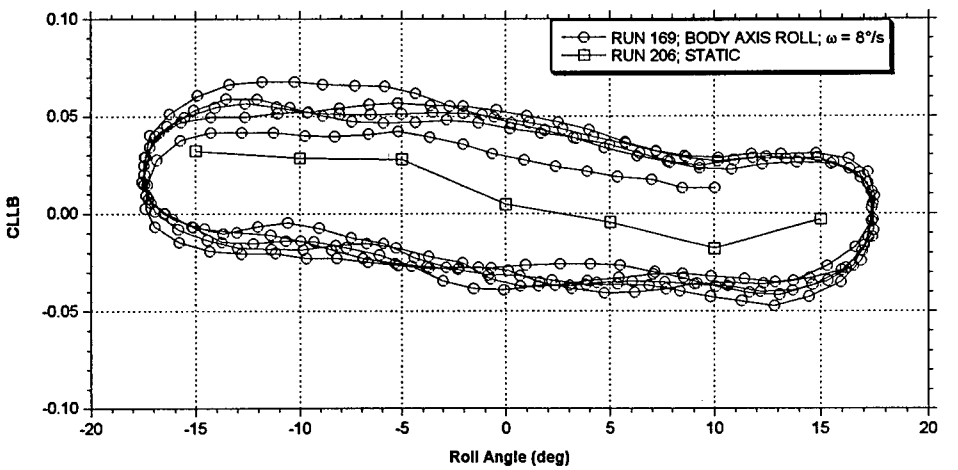

Figure 15 - F/A-18 (1/48 scale) Body Axis Roll Oscillation

The final set of figures, Figures 16 and 17, show the largest rate tested, 12°/s. In these examples, the distance between the upper and lower loops has not increased in proportion to the roll rate, indicating a "leveling-off" of the rate damping. The last figure, a larger amplitude oscillation than any of the previous examples, shows a significant decrease in the damping magnitude at large amplitudes.

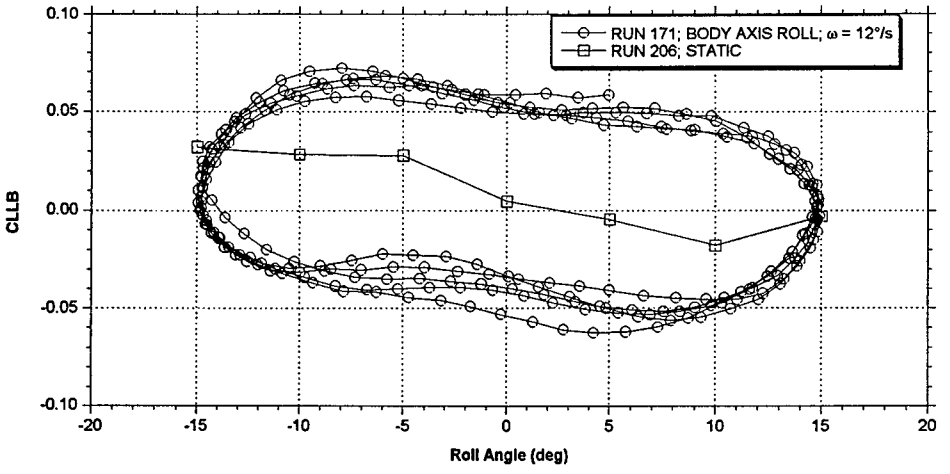

Figure 16 - F/A-18 (1/48 scale) Body Axis Roll Oscillation

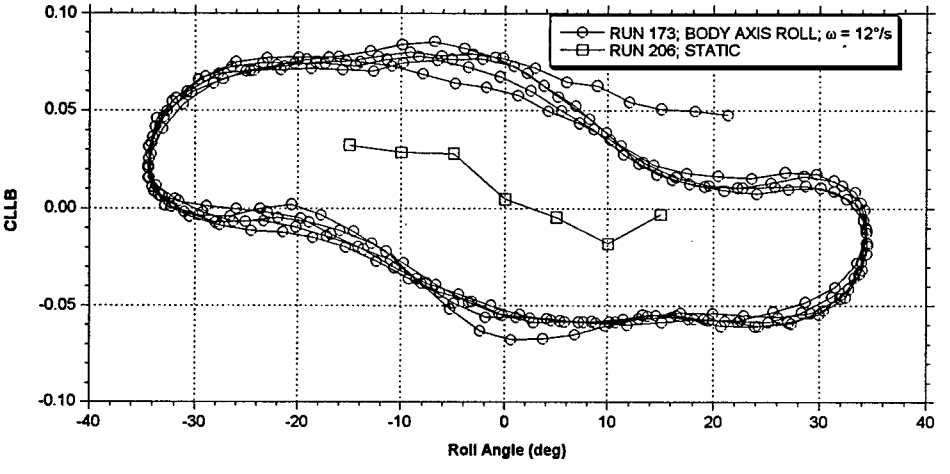

Figure 17 - F/A-18 (1/48 scale) Body Axis Roll Oscillation

7.3.2 Simple Superposition

Simple superposition refers to the decomposing of an arbitrary rotation into three (or two in the symmetric case) orthogonal components. For example, a rotation Ω in the symmetry plane can be expressed as the sum of two body axis rotations p and r. A simple vector diagram illustrates this.

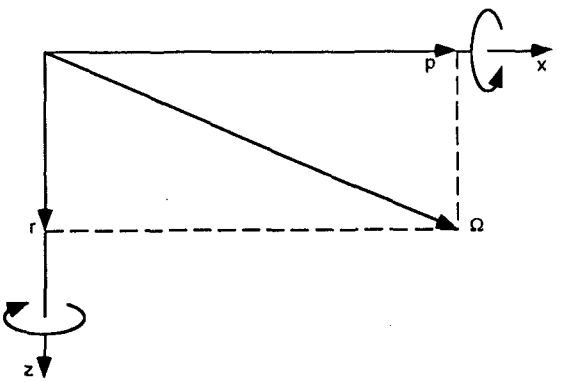

The decomposition of the motion can be written as a vector equation, $\vec{\Omega} = \vec{p} + \vec{r}$. The superposition assumption comes in when the aerodynamic contributions due to p and r rotations are assumed to be independent and additive, that is $C_k(\Omega) = C_k(p) + C_k(r)$.

This type of superposition is commonly used when rotary balance data is unavailable. Small amplitude, forced-oscillation tests would supply the rate dependent aerodynamic data.

Simple superposition can decompose any rotation into any orthogonal axis system equally. The example discussed above decomposes a roll into a body axis roll and a body axis yaw. For the purposes of performing the tests in the water tunnel, it was slightly easier to decompose a body axis roll into a wind axis roll and a wind axis yaw. This is illustrated below.

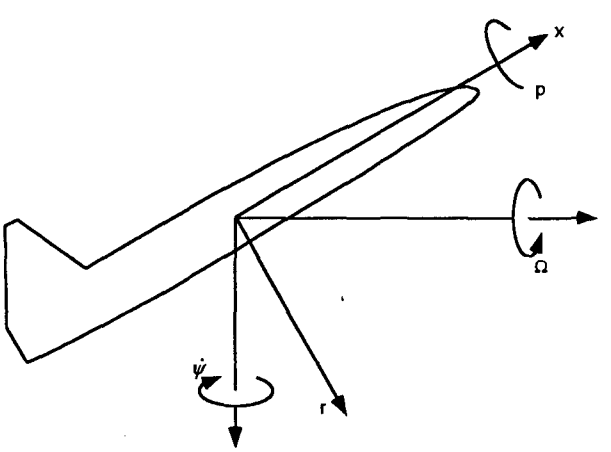

Expressed in vector notation, the motion equation is $\vec{p} = \vec{\Omega} + \vec{\dot{\psi}}$ and the corresponding aerodynamic addition becomes $C_k(p) = C_k(\Omega) + C_k(\dot{\psi})$.

The example shown from the experimental investigation is a body axis roll oscillation at a nominal angle of attack of 40°. The particulars of the body axis roll motion and its equivalent wind axis roll and yaw components are listed in the table below. Notice that each of the oscillations has the same period.

α=40°	Body Axis	Wind Axis Equivalent	
	Roll	**Roll**	**Yaw**
Angular Rate	**15.7°/s**	**12.0°/s**	**-10.1°/s**
Period	**10 sec**	**10 sec**	**10 sec**
Amplitude	**± 39.2°**	**± 30.0°**	**± 25.2°**
Run #	**173**	**120**	**134**

Figure 18 shows the rolling moment response for the body axis roll oscillation. This is actually the same run as was shown in the previous discussion regarding roll amplitude effects. Figures 19 and 20 show the roll moment developed for the component motions in the wind axis. The dynamic response of the yaw oscillation is much larger than that of the roll motion, indicating that most of the roll damping shown in the body axis roll is developed as a result of the wind axis yaw motion. This observation is sensible since a wind axis roll largely takes place at a constant angle of attack and sideslip, whereas during a wind axis yaw the sideslip angle changes radically.

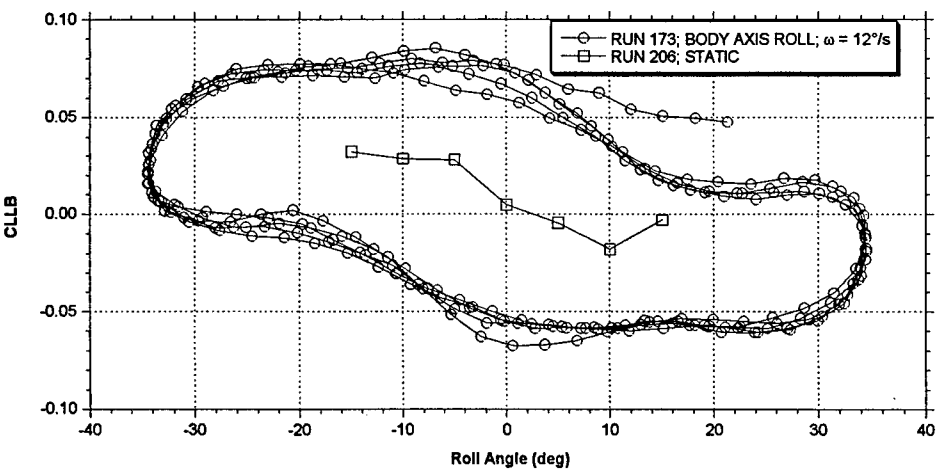

Figure 18 - F/A-18 (1/48 scale) Body Axis Roll Oscillation

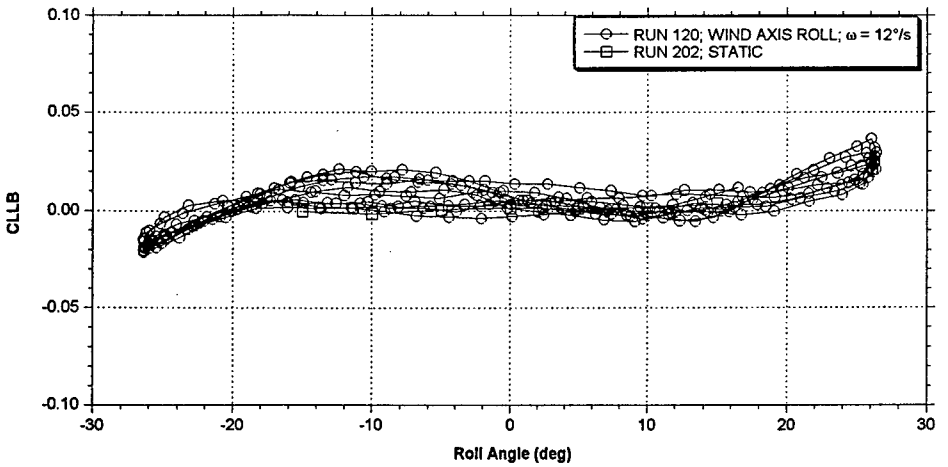

Figure 19 - F/A-18 (1/48 scale) Wind Axis Roll Oscillation

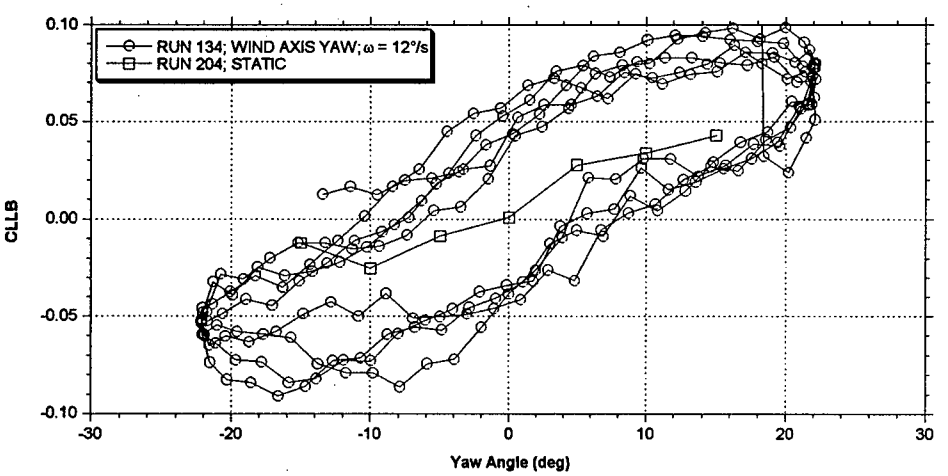

Figure 20 - F/A-18 (1/48 scale) Wind Axis Yaw Oscillation

The scatter in the measured data during the yaw oscillation shown in Figure 20 is a direct result of the resonant frequency of the model support structure being excited by roughness in the yaw turntable. The weak section of the structure has been identified and is being redesigned.

7.3.3 Rotation Axis near Velocity Vector

The simple superposition method, described above, is often used when rotary balance data is not available. Simple superposition decomposes an arbitrary rotation into a unique combination of rotations about three orthogonal vectors, generally, body axis rotations. Rotary balance tests rotate around the velocity vector, which obviously is not orthogonal to the body axes. The addition of rotary balance data complicates the

decomposition process, but should provide better estimates of the dynamic aerodynamics during an arbitrary motion.

Two common decomposition techniques will be applied to two flight conditions that should highlight the differences in the schemes. The methods will be referred to as the "Conventional" method and the "Kalviste" method. Both can be applied to three dimensional maneuvers, but for the purposes of this discussion, only symmetric maneuvers will be examined. The first motion will be an oscillation about an axis 10° above the velocity vector. The nominal angle of attack is 40°.

Conventional Superposition

Conventional superposition starts with the tacit assumption that most motions are primarily velocity vector rolls, and as a result, decomposes all motions into a wind axis roll with the smallest possible adjustment with residual body axis components. Generally, the aerodynamic contribution from the wind axis roll is obtained through rotary balance tests, while the body axis components come from small amplitude forced oscillation tests. The decomposition of the instantaneous motion can be expressed as a vector equation, $\vec{\Omega} = \vec{\mu} + \vec{p} + \vec{r}$. The corresponding aerodynamic build-up is then $C_k(\Omega) = C_k(\mu) + C_k(p) + C_k(r)$. The vector diagram below shows the Conventional method decomposition of an 8°/s rotation about an axis 10° above the velocity vector (λ=10°) at a nominal angle of attack of 40°.

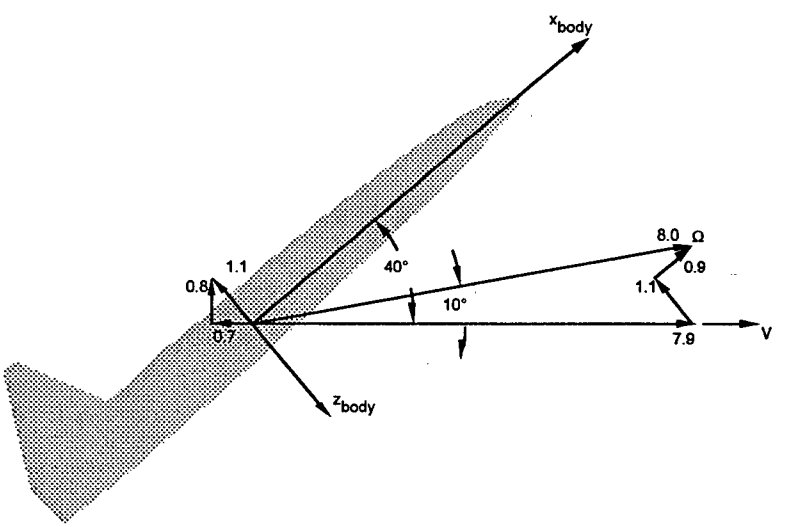

The particulars for the experimental example are tabulated below.

α=40° λ=10°	Complete Motion	Component Motions via Conventional Method		
	Roll about Inclined Axis	**Wind Axis Roll**	**Body Axis Roll**	**Body Axis Yaw**
Angular Rate	**8.0°/s**	**7.9°/s**	**0.9°/s**	**-1.1°/s**
Period	**5 sec**	**5 sec**	**5 sec**	**5 sec**
Amplitude	**± 10.0°**	**± 9.8°**	**± 1.1°**	**± 1.3°**
Run #	**187**	**191**	**179**	**199**

Performance of a body axis yaw oscillation was required to complete the decomposition of the inclined axis roll. This motion would be very difficult, if not impossible, to obtain with a typical wind tunnel model support system. However, in the water tunnel it is simply a matter of programming simultaneous oscillations of wind axis roll and yaw. The vector diagram shows this vector sum as well.

Figure 21 shows the yaw moment measured during the inclined axis test. The oscillation was performed for multiple cycles as in the early experiments, but for clarity, only a single representative cycle is plotted here. The amplitude has been non-dimensionalized on the abscissa to allow easier comparison between the plots. Figures 22 through 24 show the measured yaw moment resulting from each of the component motions. The dominate role of the wind axis roll component can be readily discerned.

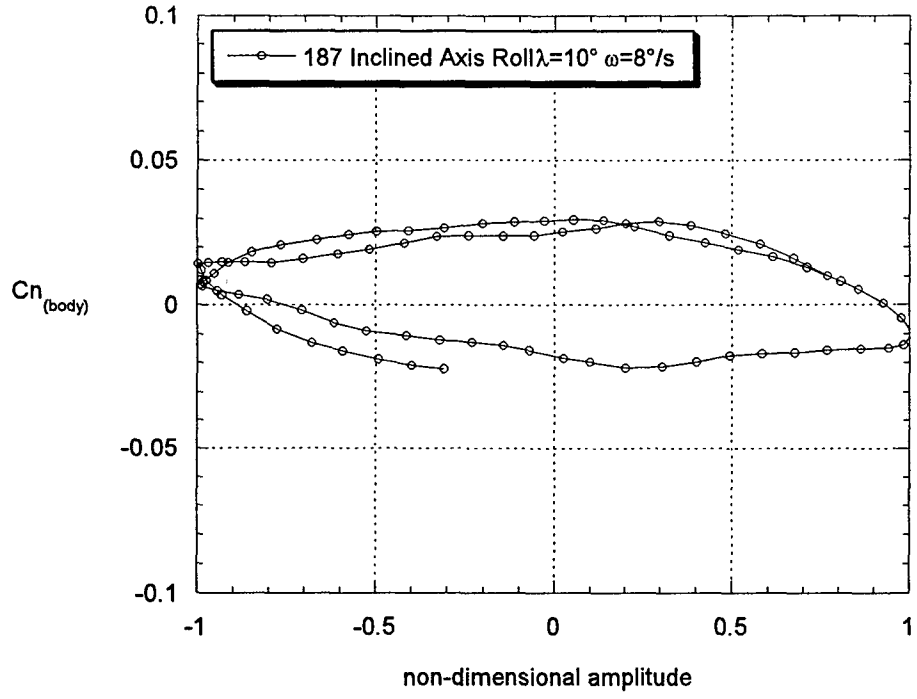

Figure 21 - F/A-18 (1/48 scale) Inclined Axis Roll Oscillation

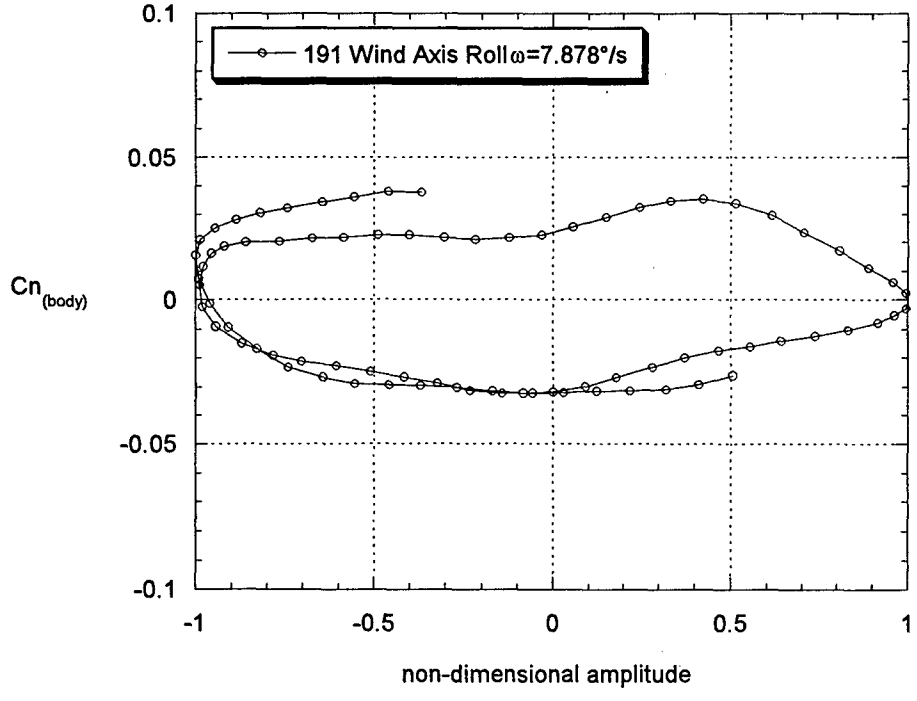

Figure 22 - F/A-18 (1/48 scale) Wind Axis Roll Oscillation Conventional Build-up Method

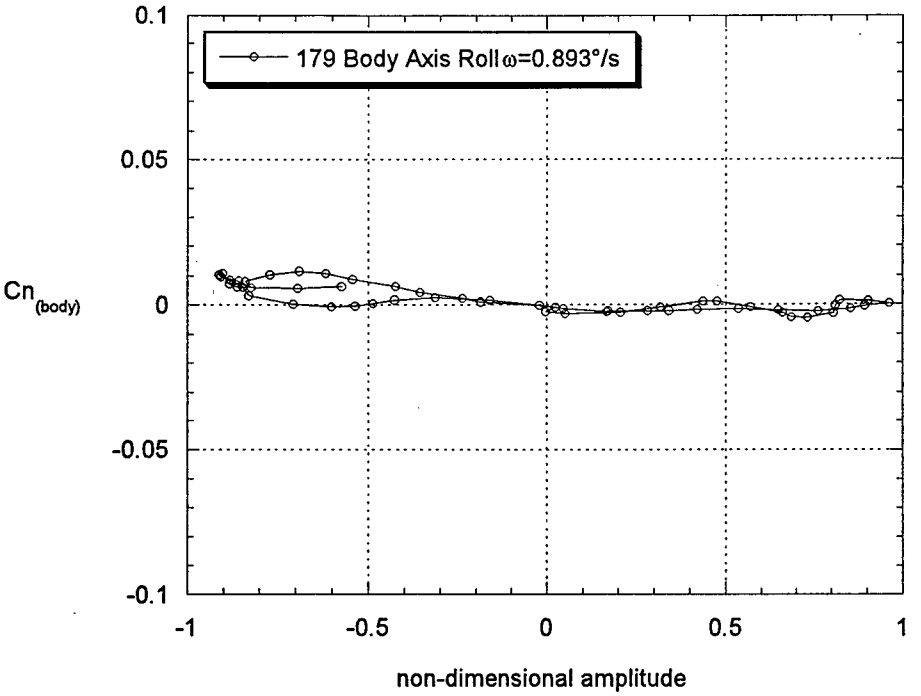

Figure 23 - F/A-18 (1/48 scale) Body Axis Roll Oscillation Conventional Build-up Method

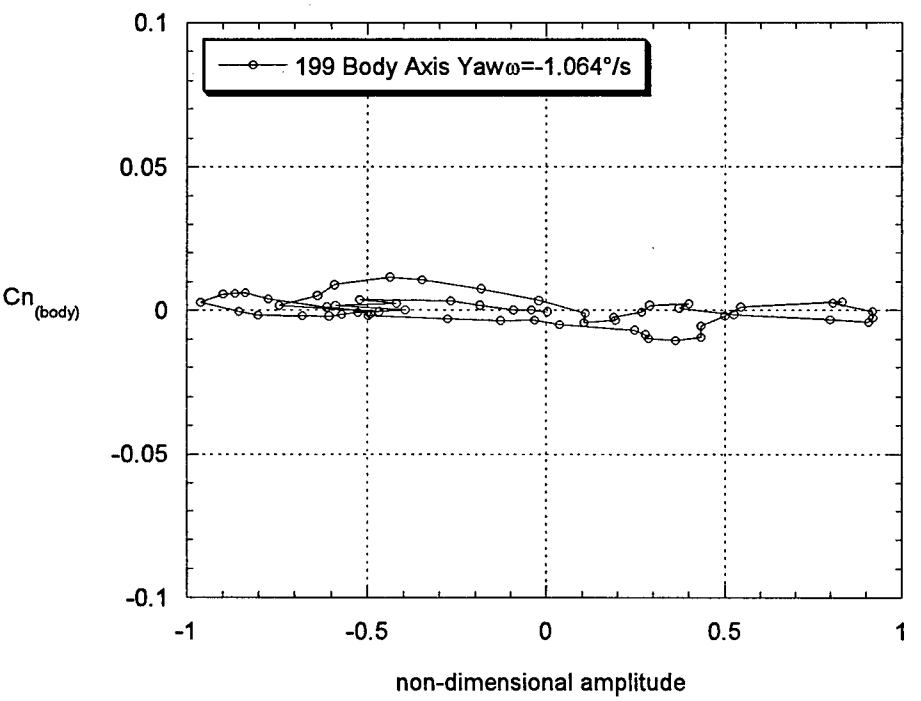

Figure 24 - F/A-18 (1/48 scale) Body Axis Yaw Oscillation Conventional Build-up Method

Juri Kalviste's Superposition

Juri Kalviste developed a different method that uses the component vectors "closest" to the instantaneous motion to decompose the motion. For the symmetric motion of the previous example, the rotation vector falls between the wind axis and the body roll axis, so these two are selected. The vector diagram shows the decomposition.

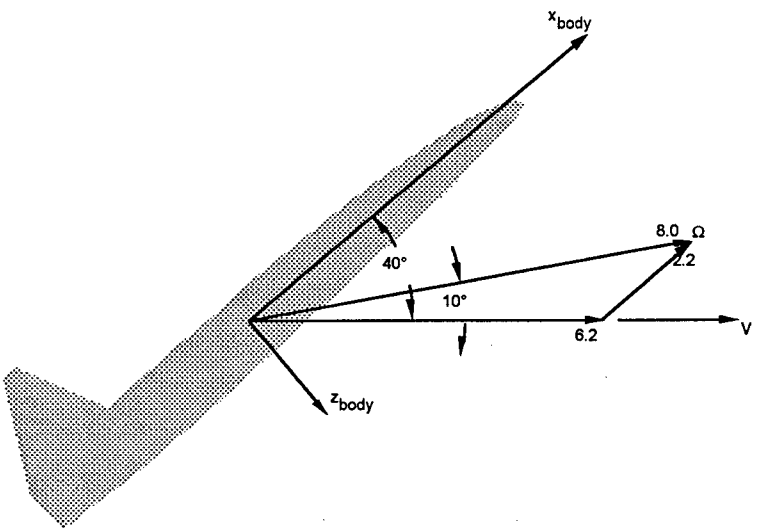

The vector sum for this case is: $\vec{\Omega} = \vec{\mu} + \vec{p}$ and the aerodynamic build-up is $C_k(\Omega) = C_k(\dot{\mu}) + C_k(p)$.

The details of the experiments are given in the table below.

α=40° λ=10°	Complete Motion	Component Motions via Kalviste Method	
	Roll about Inclined Axis	**Wind Axis Roll**	**Body Axis Roll**
Angular Rate	**8.0°/s**	**6.2°/s**	**2.2°/s**
Period	**5 sec**	**5 sec**	**5 sec**
Amplitude	**± 10.0°**	**± 7.8°**	**± 2.7°**
Run #	**187**	**189**	**175**

Figure 25 repeats the yaw moment data for the inclined axis oscillation, while Figures 26 and 27 show the individual contributions. As in the previous example, the dominance of the wind axis roll is seen. This is not too surprising, given that the motion is fairly close to a velocity vector roll.

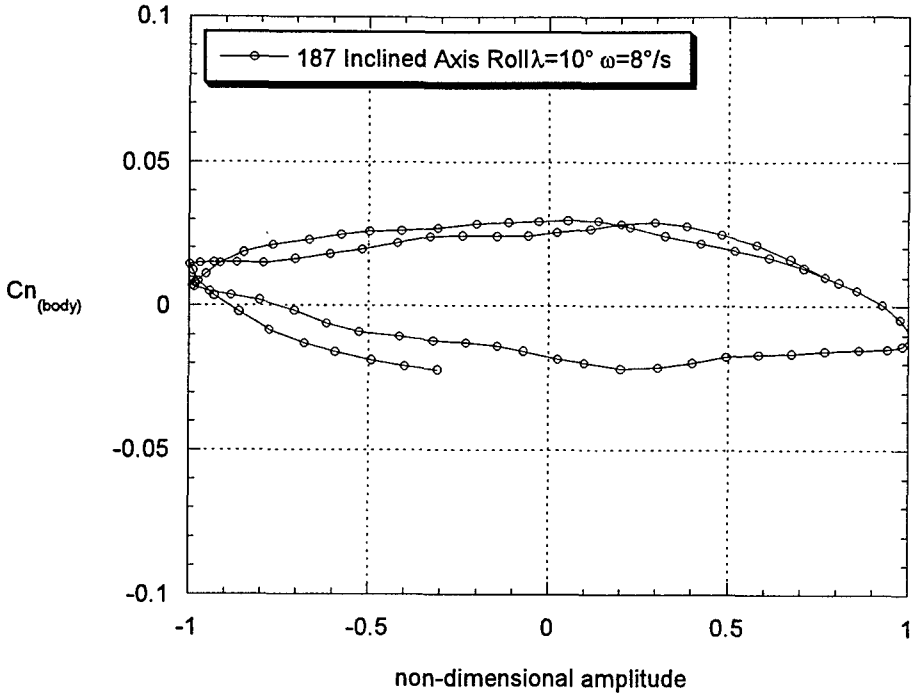

Figure 25 - F/A-18 (1/48 scale) Inclined Axis Roll Oscillation

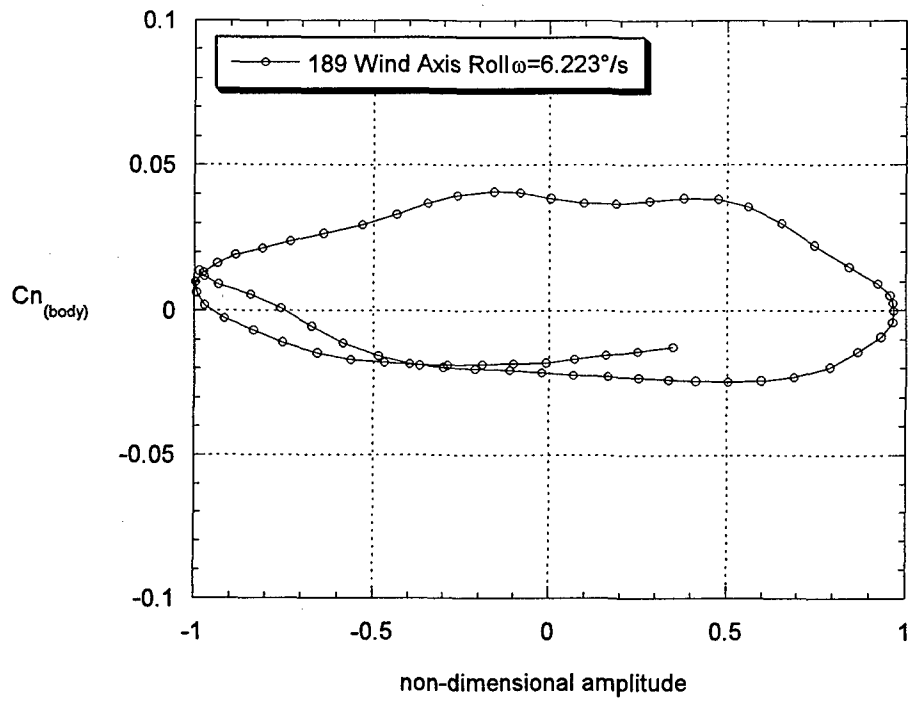

Figure 26 - F/A-18 (1/48 scale) Wind Axis Roll Oscillation Kalviste Build-up Method

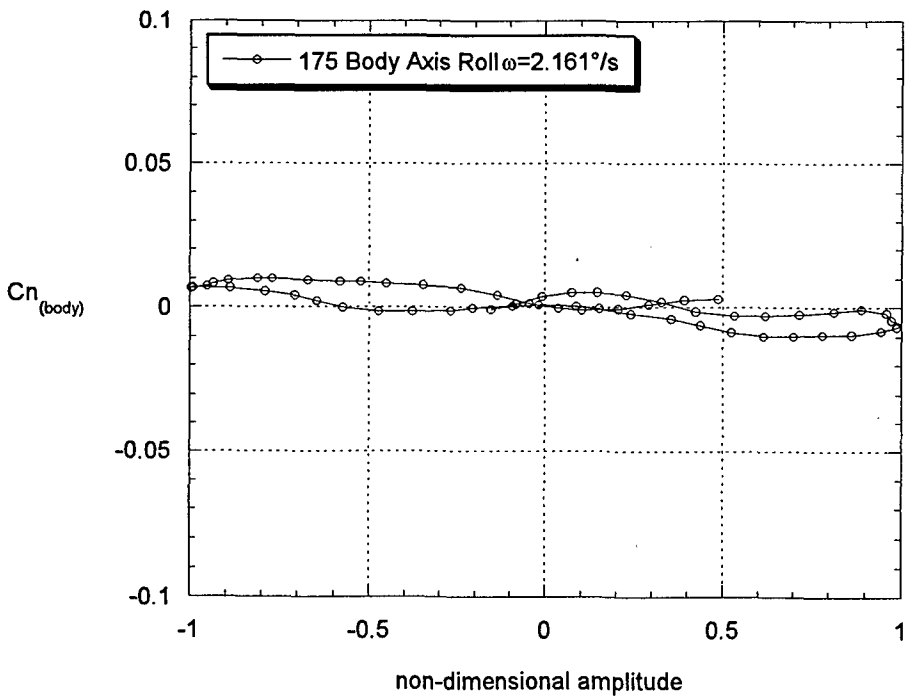

Figure 27 - F/A-18 (1/48 scale) Body Axis Roll Oscillation Kalviste Build-up Method

7.3.4 Rotation Axis near Body Roll Axis

The second example motion should highlight the differences between the two decomposition methods. This example will again be at a nominal angle of attack of 40°, but the rotation axis will be 10° below the body roll axis, or 30° above the velocity vector (λ=30°).

Conventional Superposition

The conventional method always uses the smallest possible correction to the wind axis roll vector, so even in a case such as this where the rotation axis is close to the body axis, there will be a significant portion of the motion allocated to the wind axis roll and a relatively small amount to body axis roll. In addition, body axis yaw will have a fairly large share of the motion. The vector diagram and tabulated values show the relative magnitudes of the vectors.

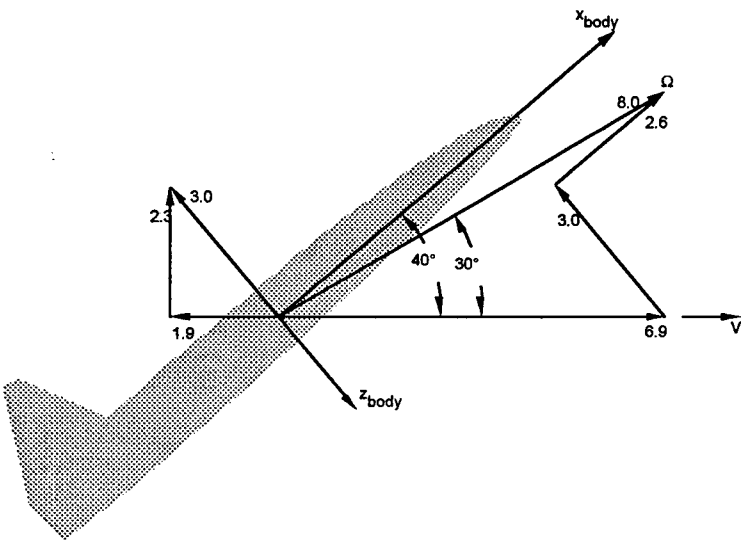

α=40° λ=30°	Complete Motion	Component Motions via Conventional Method		
	Roll about Inclined Axis	**Wind Axis Roll**	**Body Axis Roll**	**Body Axis Yaw**
Angular Rate	**8.0°/s**	**6.9°/s**	**2.6°/s**	**-3.1°/s**
Period	**5 sec**	**5 sec**	**5 sec**	**5 sec**
Amplitude	**± 10.0°**	**± 8.7°**	**± 3.2°**	**± 3.8°**
Run #	**185**	**195**	**183**	**197**

Figure 28 shows the total yaw moment response due to the inclined axis roll oscillation. Similar to other plots shown previously, the motion progress counterclockwise around the loop indicating that the oscillation has positive damping. Figures 29 through 31 show the aerodynamic effects of each of the component motions. Each of these loops are also traversed in a counterclockwise direction. A cursory visual inspection clearly shows that the wind axis roll oscillation, Fig. 29, develops more yaw damping than the inclined roll, and each of the other motions add even more damping. Based on the data shown here, it appears that the conventional method has failed in this case to adequately build-up the aerodynamic effects of an arbitrary motion. Furthermore, doubt is cast on the applicability of the superposition assumption.

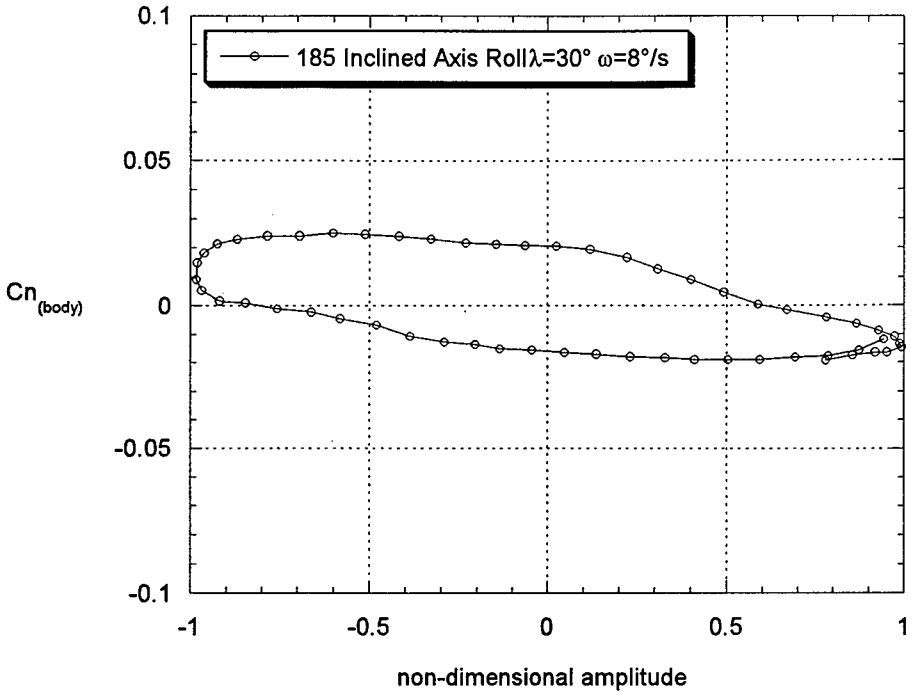

Figure 28 - F/A-18 (1/48 scale) Inclined Axis Roll Oscillation

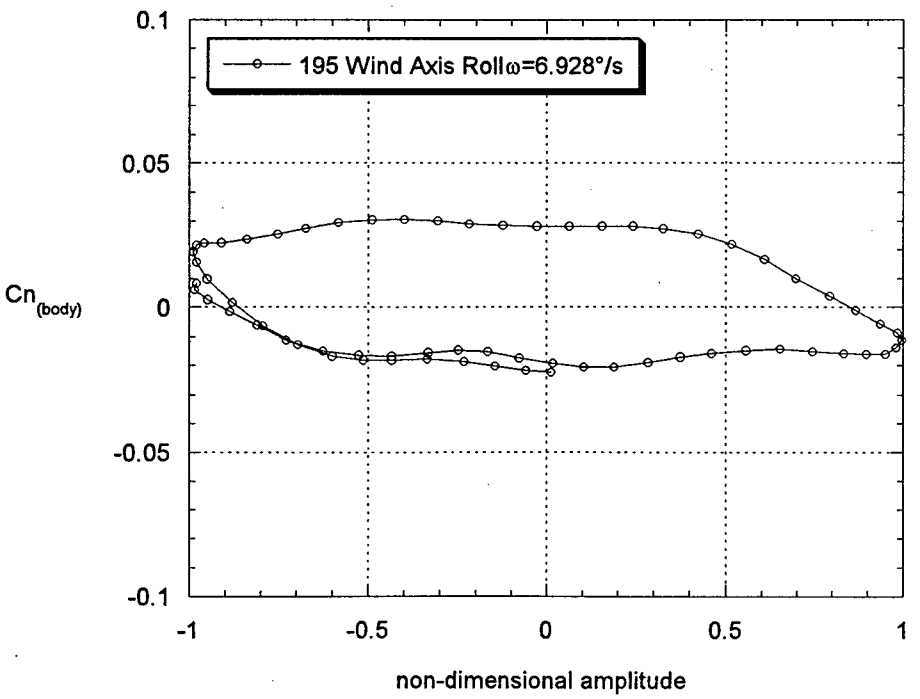

Figure 29 - F/A-18 (1/48 scale) Wind Axis Roll Oscillation Conventional Build-up Method

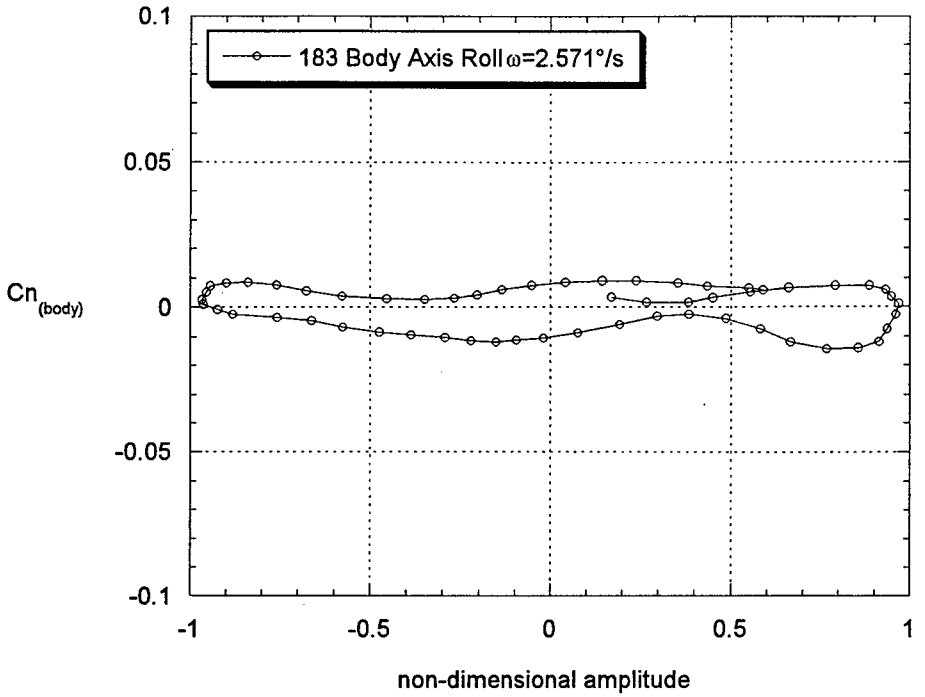

Figure 30 - F/A-18 (1/48 scale) Body Axis Roll Oscillation Conventional Build-up Method

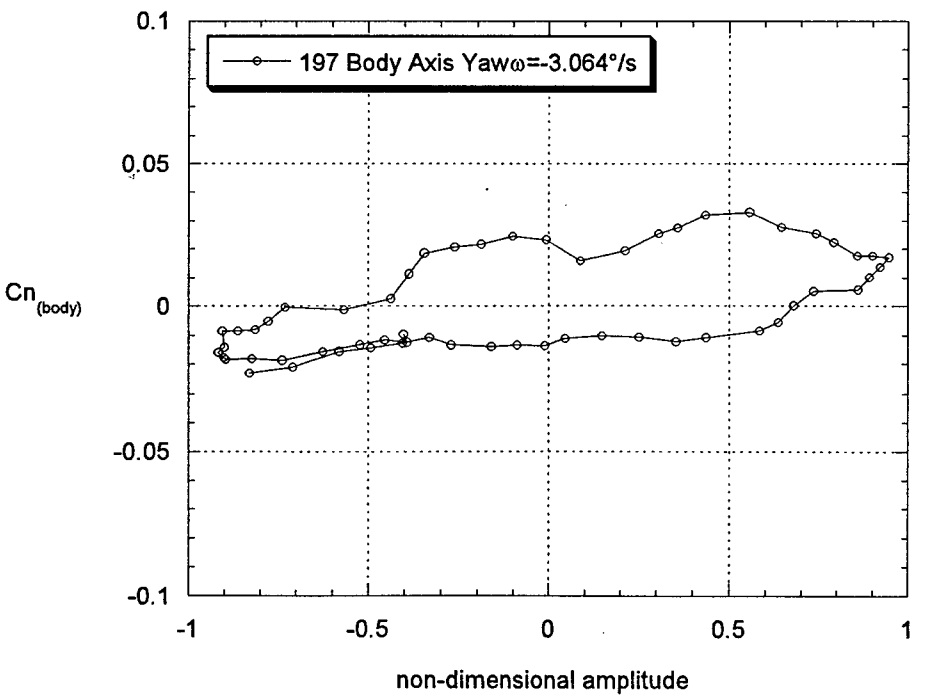

Figure 31 - F/A-18 (1/48 scale) Body Axis Yaw Oscillation Conventional Build-up Method

Juri Kalviste's Method

It was because of the perceived inadequacies of the conventional method to model motions that involve rotation axes far remove from the velocity vector, that prompted Kalviste to develop his alternative method. In fact, if the rotation axis coincided with the body x-axis, the Kalviste method will return the body axis roll aerodynamics. This is not true of the conventional method (unless, the superposition principle held exactly).

The Kalviste decomposition of the second inclined axis example is shown in the now familiar vector diagram and table below. Notice that the component motions are largely a body axis roll with a moderate wind axis roll rotation. The Kalviste method, produces component vectors that are more closely aligned with the total motion than the conventional method.

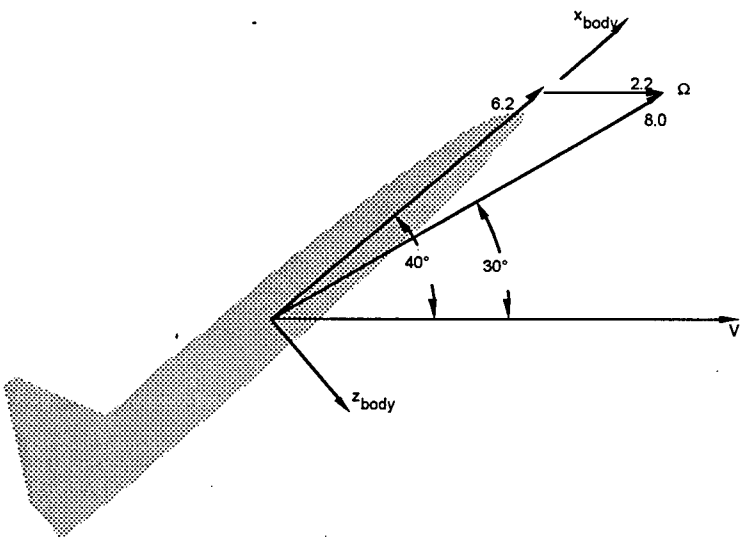

α=40° λ=30°	Complete Motion	Component Motions via Kalviste Method	
	Roll about Inclined Axis	**Wind Axis Roll**	**Body Axis Roll**
Angular Rate	**8.0°/s**	**2.2°/s**	**6.2°/s**
Period	**5 sec**	**5 sec**	**5 sec**
Amplitude	**± 10.0°**	**± 2.7°**	**± 7.8°**
Run #	**185**	**193**	**177**

Figure 32 repeats the aerodynamic response of the λ=30° inclined axis oscillation. Figures 33 and 34 show the effects of the component motions. As in all the previous examples, the loops are counterclockwise, indicating positive yaw damping and are additive. More analysis is necessary to evaluate whether the superposition principle is valid. However, in this case, the Kalviste method does a better job of producing the correct aerodynamic build-up.

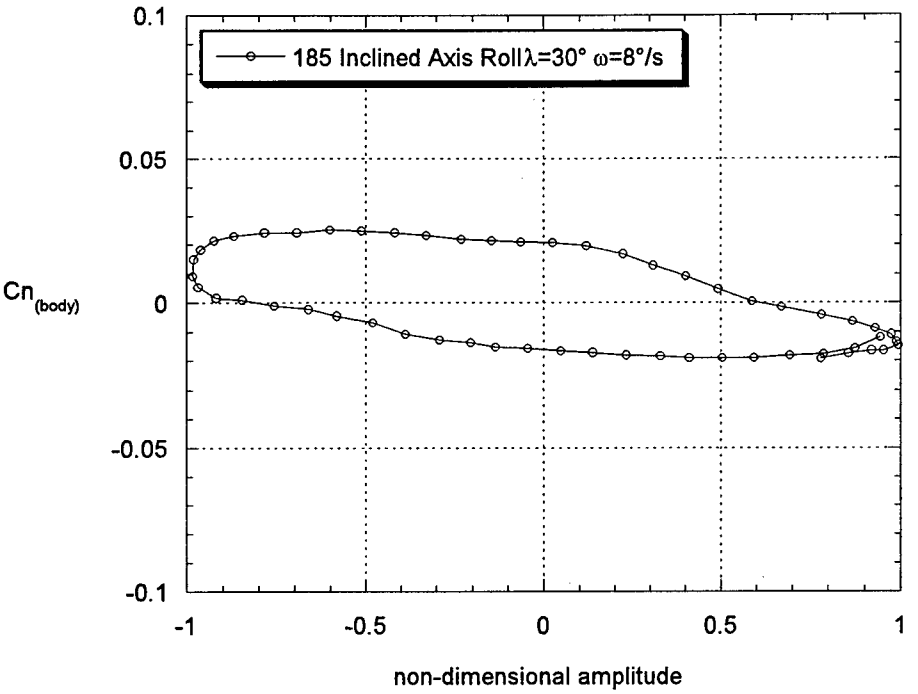

Figure 32 - F/A-18 (1/48 scale) Inclined Axis Roll Oscillation

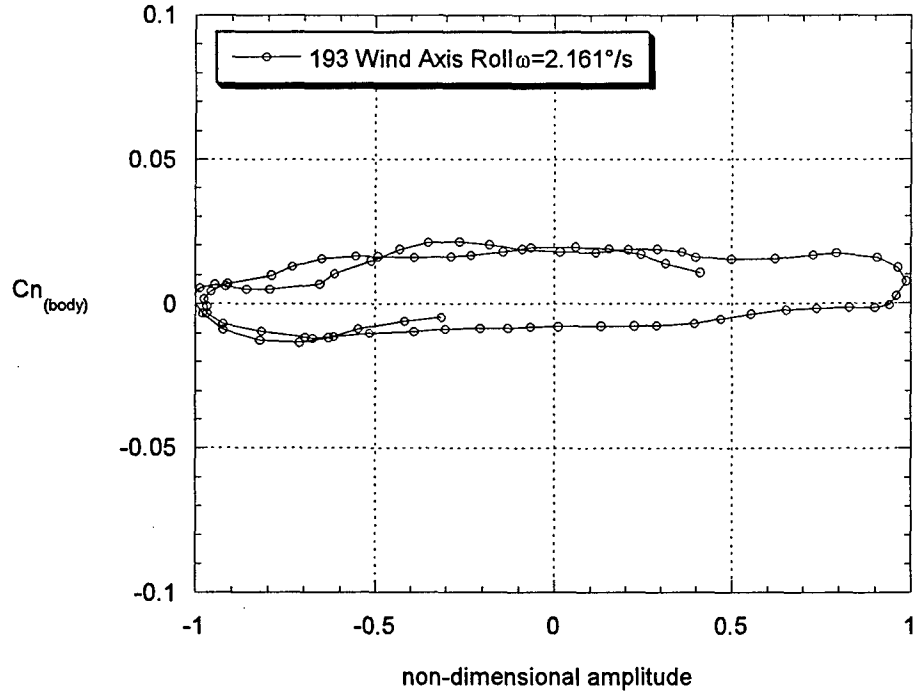

Figure 33 - F/A-18 (1/48 scale) Wind Axis Roll Oscillation Kalviste Build-up Method

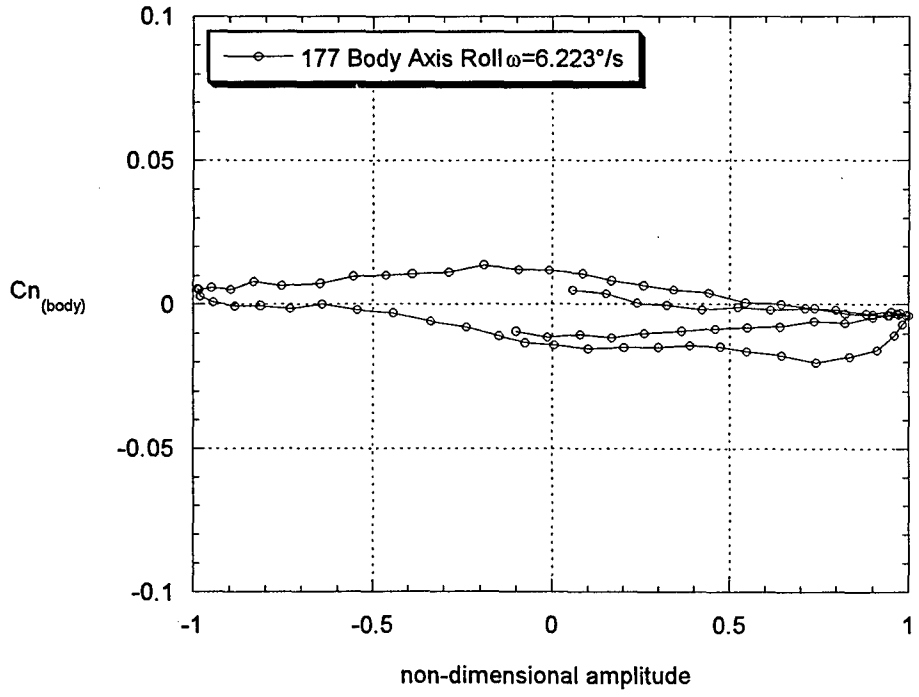

Figure 34 - F/A-18 (1/48 scale) Body Axis Roll Oscillation Kalviste Build-up Method

7.3.5 Other Experiments

The unique capability afforded by water tunnel dynamic tests allows many other experiments investigating other nonlinear dynamic phenomena. For example:

- pitch oscillations about different rotations centers to separate pitch rate effects from angle of attack rate effects.
- Oscillations at lower angles of attack where vortex burst locations become significant.
- Oscillations at different frequencies for the extraction of aerodynamic transfer functions.
- Flow visualization in conjunction with force measurements to allow the correlation of critical states to changes in flow field topology.
- Ramp and hold motions to identify aerodynamic time lag and overshoot responses and separate damping due to lag from damping due to rate.

7.4 Conclusions from Experimental Investigation

Model motions impossible to produce in a wind tunnel are easily obtainable in the water tunnel. This is due to the very small inertia effects, low rotational rates, and light weight models made possible by the water tunnel test environment. However, this investigation also revealed some areas in the model support system that could benefit from improvement. These include increasing the rigidity of some elements in the support structure, providing for a smoother yaw motion, and upgrades to the motion control firmware to allow motions with time-varying accelerations.

The internal, submersible balance has demonstrated the sensitivity required to resolve and extract dynamic, time varying, aerodynamic effects in the water tunnel. Improvements to the balance design and data acquisition system will increase the signal-to-noise ratio and improve the data quality. Changes to the data acquisition and tunnel operation software will increase the automation of the dynamic testing procedures and streamline testing.

The viability and utility of the water tunnel as a dynamic test facility and research tool for nonlinear aerodynamics has been established. The unique test capability afforded by the water tunnel can go beyond what is possible in any wind tunnel facility. In addition, the flow visualization ability in conjunction with

accurate force measurements offers tantalizing possibilities in the realm of indicial response theory and the identification of critical states and bifurcations.

Based on the data presented, superposition of dynamic aerodynamic effects may not be a valid assumption. This could have dramatic impact on the methods that nonlinear dynamic aerodynamic models are formulated and used. More investigation is required.

8.0 CONCLUDING REMARKS

With a thorough review of present-day, typical dynamic test techniques used in wind tunnels around the world, it is obvious that there are serious shortcomings in the ability to properly measure and model the dynamic aerodynamic coefficients that will represent fighter aircraft at high angles of attack, where there are significant nonlinearities in the aerodynamics data and non-neglible motion time-history effects.

The water tunnel tests have shown the potential to provide measurements of dynamic force and moment quantitites with motions that cannot be provided in wind tunnel tests. Because the models have low inertia and the water tunnel velocity is very low resulting in low model rotation rates for proper scaling, it becomes possible to generate motions in 1 to 3 rotational axes simultaneously and to measure the model forces and moments simultaneously with flow visualization. In addition to the ability to measure dynamic forces and moments in real time (properly scaled), it is also possible to determine where "critical flow states" exist with static tests. These critical flow state experiments help to promote guidance for establishing the test boundaries for dynamic tests. These critical flow states typically occur as a result of vortex breakdown and the proximity of the vortex burst dynamics to lifting surfaces such as the wing or wing leading-edge extension and the vertical tail (for yaw effects).

The approach for future testing is to constrain the classical small-amplitude forced-oscillation tests to the angle of attack regime where the aerodynamics can still be obtained reliably without the need and assumption of linearity with rotation rate . Where critical areas are discovered, the boundaries of the area to be tested for nonlinear or time-history effects can be defined, and the areas between them can be specified as regions for classical oscillatory experiments or for non-typical type tests including real-time multi-axis capability. The identification of flow regimes will help to avoid performing dynamic experiments in the vicinity of discontinuities and abrupt changes in the value of the aerodynamics model.

9.0 REFERENCES

(1) AGARD Fluid Dynamics Panel Working Group 11, "Rotary-Balance Testing for Aircraft Dynamics", AGARD Advisory Report No. 265, December 1990.

(2) Kalviste, J, "Math Modeling of Aero Data for Aircraft Dynamic Motion", AIAA 94-AFM-26-7, presented at AIAA AFM Conference, August 1994

(3) Kalviste, J., "Use of Rotary-Balance and Forced-Oscillation Test Data in a Six Degree ofFreedom Simulation", AIAA Paper 82-1364, August 1982.

(4) Kalviste, J., "Aircraft Stability Characteristics at High Angles of Attack", Dynamic Stability Parameters, AGARD Conference Proceedings No. 235, May 1978.

(5) Tobak, M. and Schiff, L. B., "Generalized Formulation of Non-linear Pitch-Yaw-Roll Coupling: Part 1 - Nonaxisymmetric Bodies", AIAA Journal, Vol. 13, No. 3, March 1975, pp. 323-326.

(6) Tobak, M. and Schiff, L. B., "Generalized Formulation of Non-linear Pitch-Yaw-Roll Coupling: Part 2 - Nonaxisymmetric Bodies", AIAA Journal, Vol. 13, No. 3, March 1975, pp. 327-332.

(7) Tobak, M. and Schiff, L. B., "On the Formulation of the Aerodynamic Characteristics in Aircraft Dynamics", NASA TR R-456, January 1976.

(8) AGARD Fluid Dynamics Panel Working Group 16, "Cooperative Programme on Dynamic Wind Tunnel Experiments for Manoeuvring Aircraft", AGARD Advisory Report No. 305, Dec. 1996.

(9) Jenkins, J. E. and Hanff, E. S., "Non-Linear Airloads Hypersurface Representation - a Time Domain Perspective", AGARD CP-497, Nov. 1991.

(10) Jenkins, J. E. and Hanff, E. S., "Non-Linear and Unsteady Aerodynamic Responses of a Rolling 65° Delta Wing, AIAA 93-3682.

(11) Huang, X. Z., Hanff, E. S., Jenkins, J. E. and Addington, G. A., "Leading-Edge Vortex Behavior on a 65° Delta Wing Oscillating in Roll", AIAA 94-3507.

(12) Hanff, E., "Dynamic Nonlinear Airloads-Representation and Measurement", AGARD CP-386, May, 1985

(13) Suarez, C. J., Ayers, B. F., and Malcolm, G. N., "Force and Moment Measurements in a Flow Visualization Water Tunnel", AIAA 94-0673, January 1994.

(14) Suarez, C. J. and Malcolm, G. N., "Dynamic Water Tunnel Tests for Flow Visualization and Force/Moment Measurements on Maneuvering Aircraft", AIAA 95-1843, June 1995.

(15) Kramer, B. R., Suarez, C. J., Malcolm, G. N. and James, K. D., "Forebody Vortex Control on an F/A-18 in a Rotary Flow Field", AIAA 94-0619, January 1994.

(16) Kramer, B. R., Suarez, C. J., Malcolm, G. N. and Ayers, B. F.,"F/A-18 Forebody Vortex Control", NASA Contractor Report CR-4582, Volumes 1 and 2, March 1994

10.0 ACKNOWLEDGMENTS

The authors of this report would like to acknowledge the significant contributions to this research program by Dr. Ernest Hanff, who was an active consultant relative to the water tunnel tests and the analysis of the results. Dr. Hanff was responsible for the advanced wind tunnel tests which focused on high-amplitude, high-rate roll oscillations of the 65° delta wing described in Section 1.4.1. Among many other interesting results his wind tunnel experiments showed the importance of identifying critical flow states prior to defining the dynamic testing matrix. Acknowledgments are also in order for Mr. Brian Kramer, who assisted with the water tunnel test and the data acquisition and reduction system.